Finite source model determinations for large magnitude earthquakes using long-period normal mode data

K. Lentas[(1)], A. M. G. Ferreira[(1)], M. Vallée[(2)], E. Clévédé[(3)]

[(1)]School of Environmental Sciences, University of East Anglia, Norwich, UK
[(2)]Géoazur, IRD, Nice, France
[(3)]Institut du Globe de Physique, Paris, France

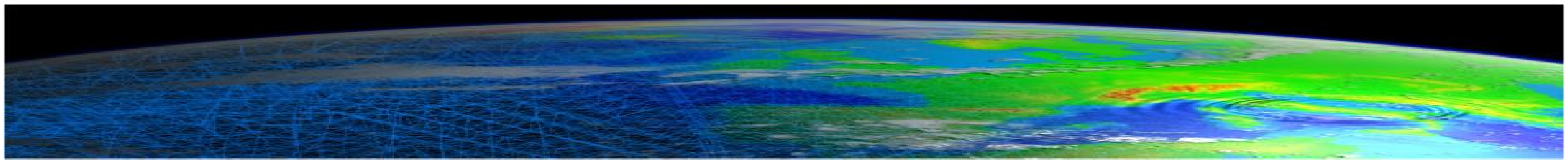

Goal and motivation

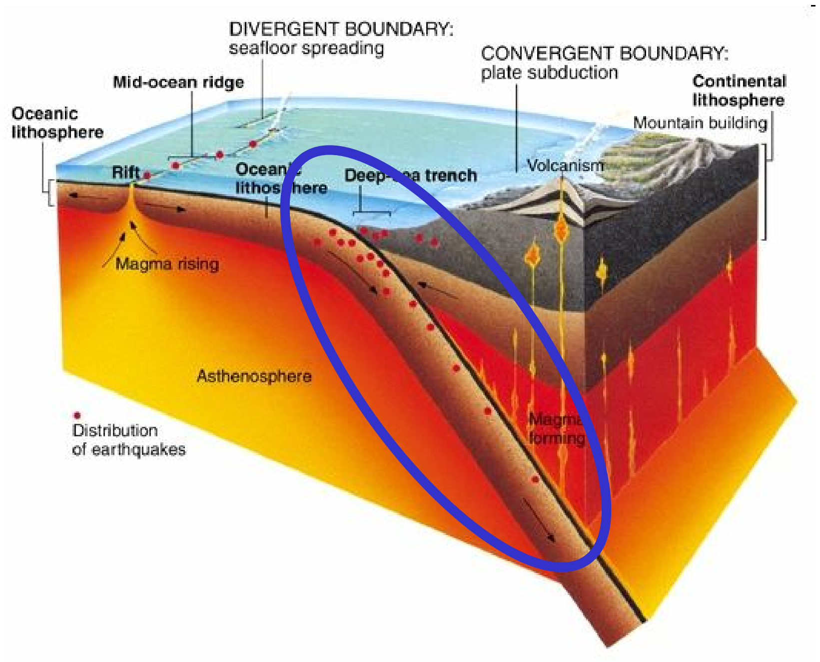

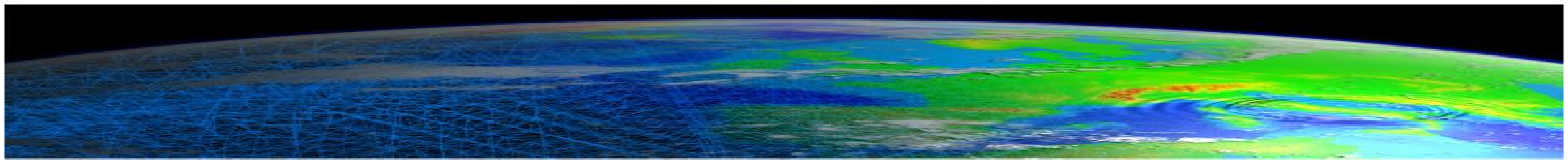

Goal and motivation

Large magnitude – shallow earthquakes

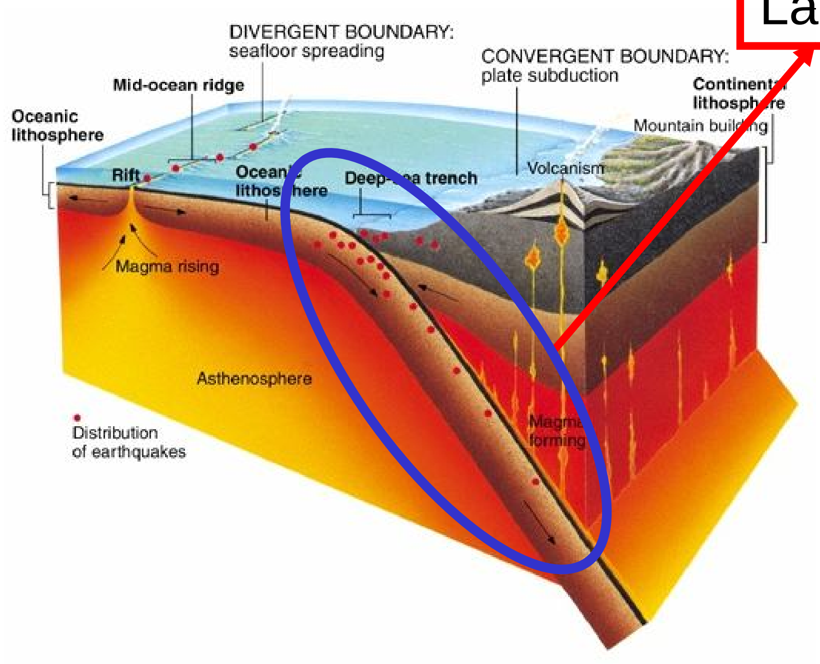

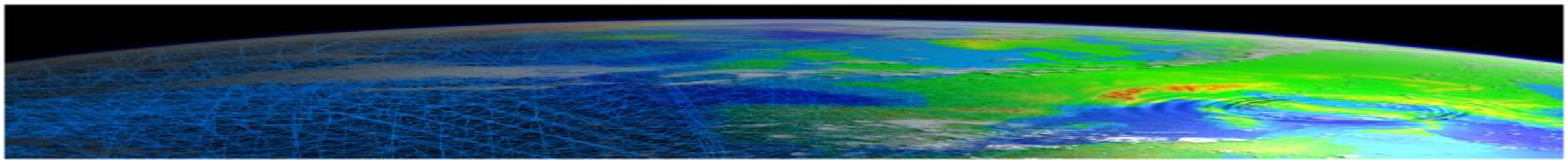

Goal and motivation

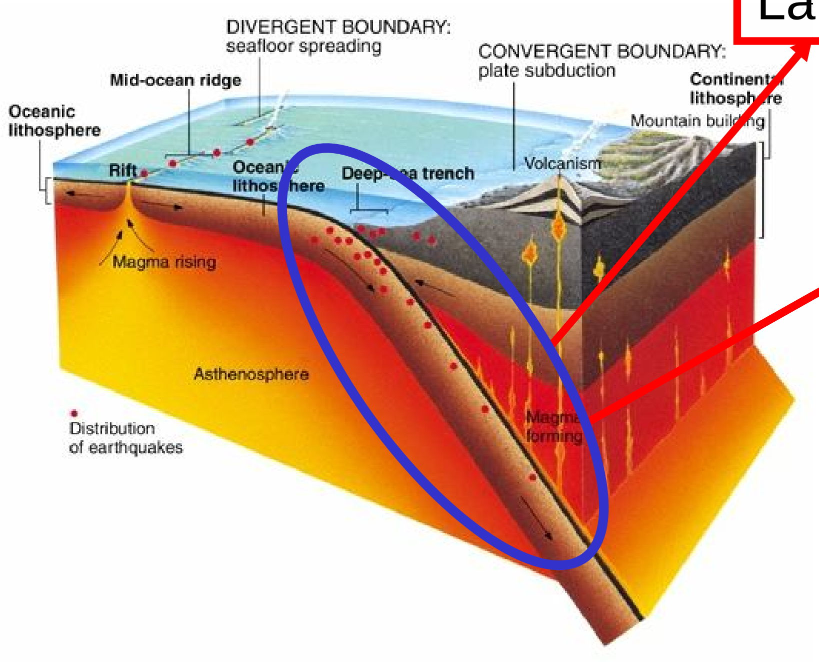

Large magnitude – shallow earthquakes

Tsunami excitation

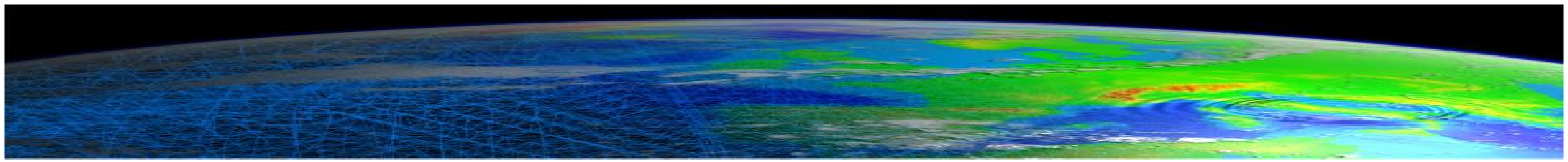

Goal and motivation

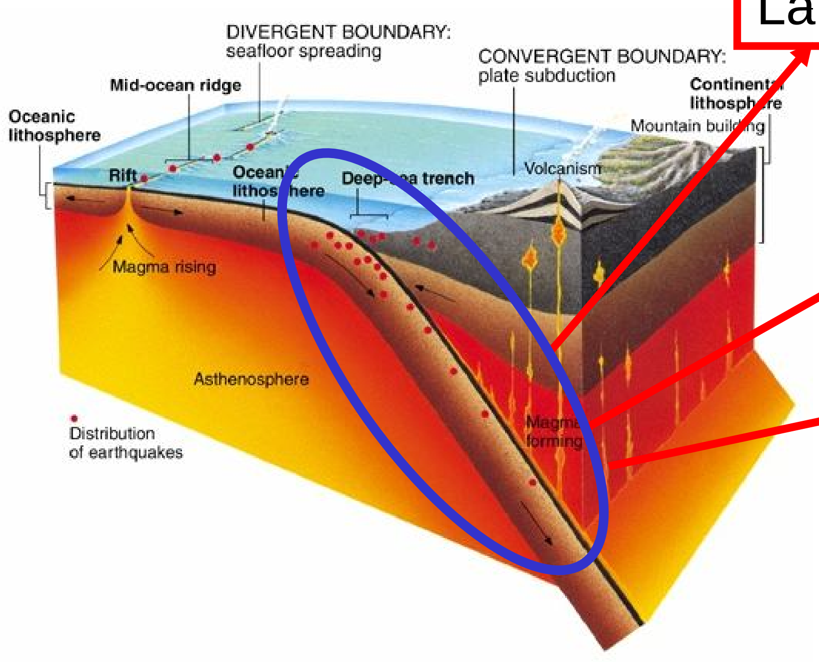

Large magnitude – shallow earthquakes

Tsunami excitation

Finite character of the source

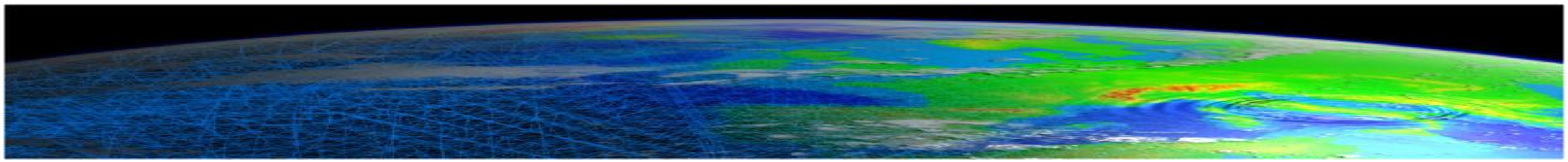

Goal and motivation

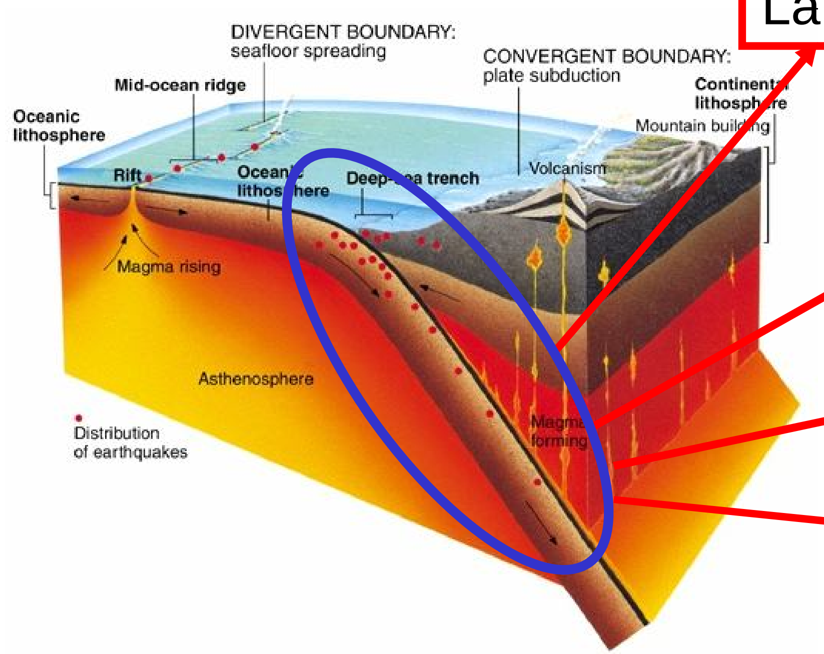

Large magnitude – shallow earthquakes

Tsunami excitation

Finite character of the source

Seismic moment – dip angle trade-off

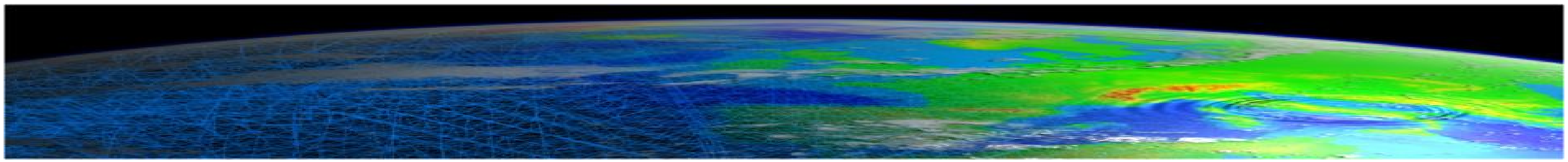

Goal and motivation

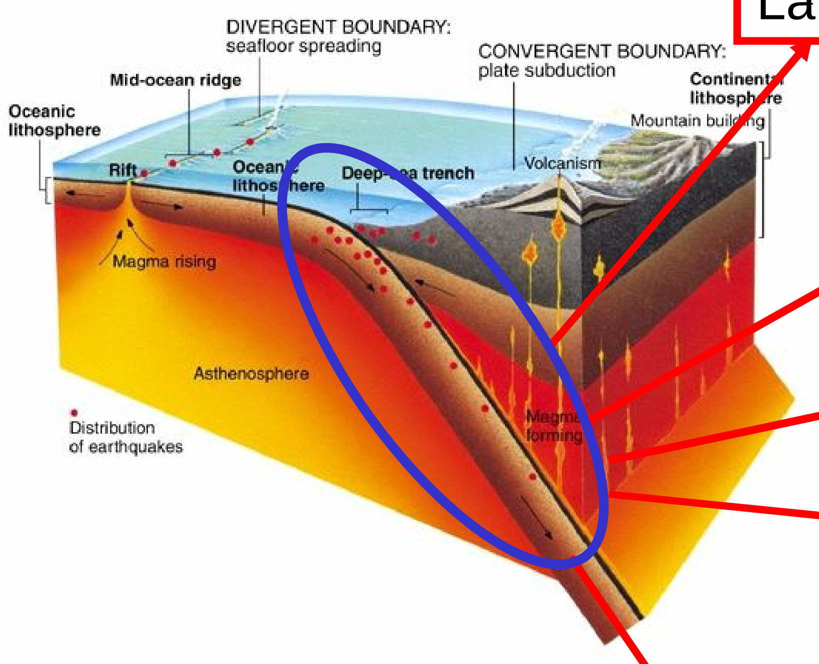

Large magnitude – shallow earthquakes

Tsunami excitation

Finite character of the source

Seismic moment – dip angle trade-off

Uncertainties

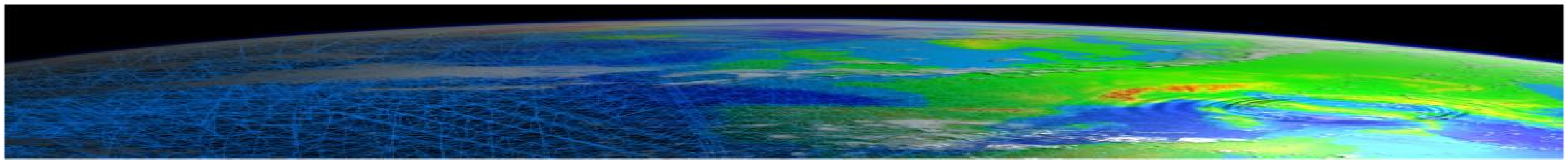

Goal and motivation

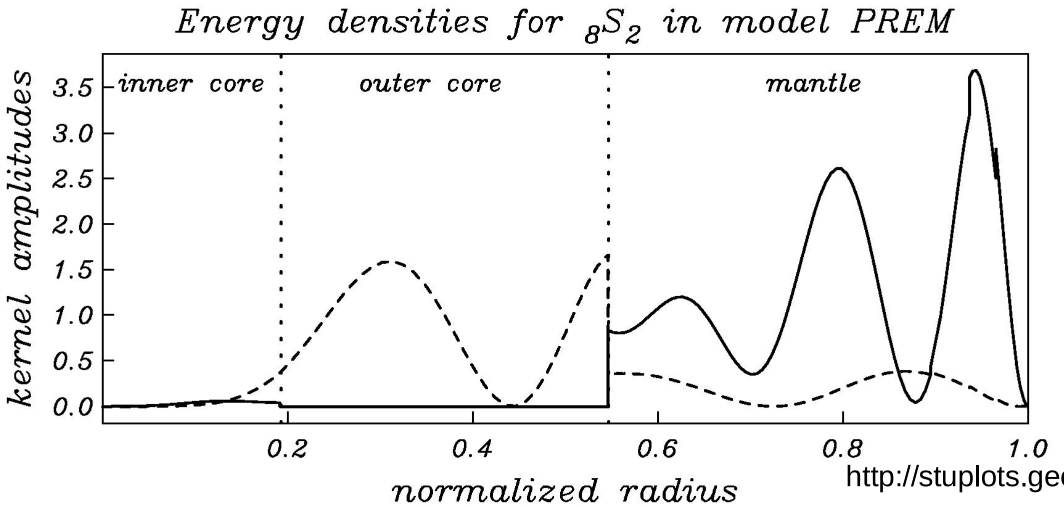

Earth's structure determination

* key factor: density (ρ)

—— shear energy density

.... compressional energy density

http://stuplots.geophys.uni-stuttgart.de/~plots/Modes/modes.html

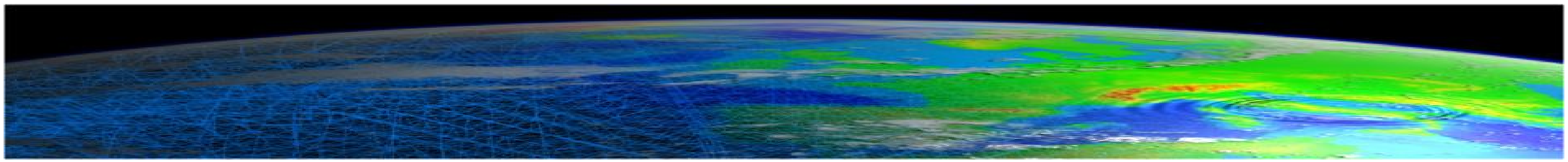

Goal and motivation

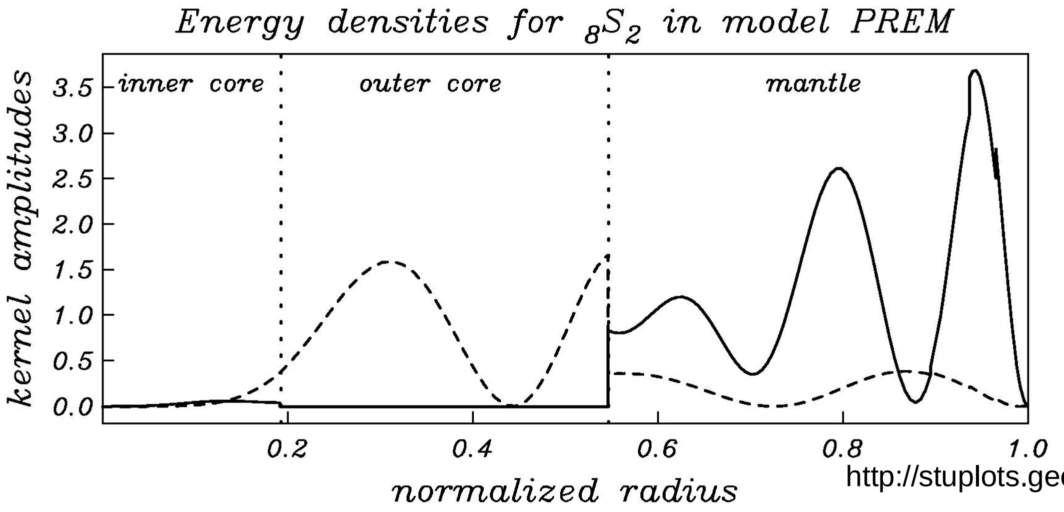

http://stuplots.geophys.uni-stuttgart.de/~plots/Modes/modes.html

Earth's structure determination

* key factor: density (ρ)

shear energy density

compressional energy density

Earthquake source studies

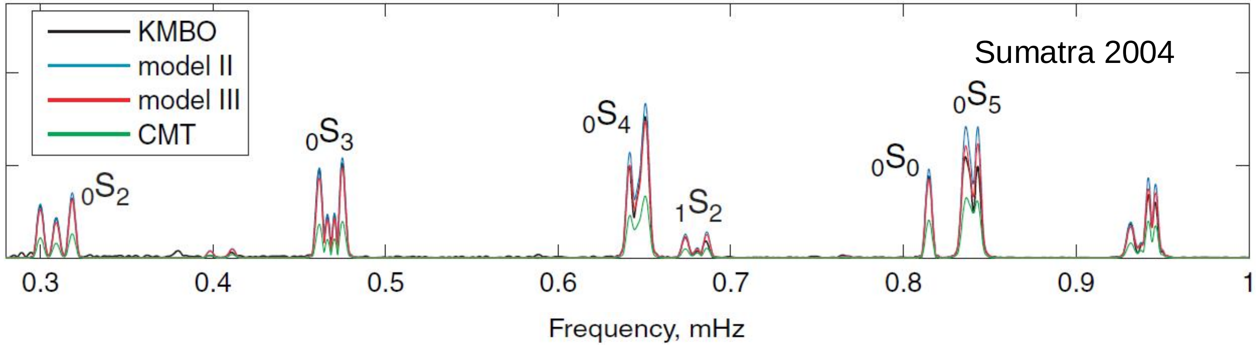

Park et al., (2005)

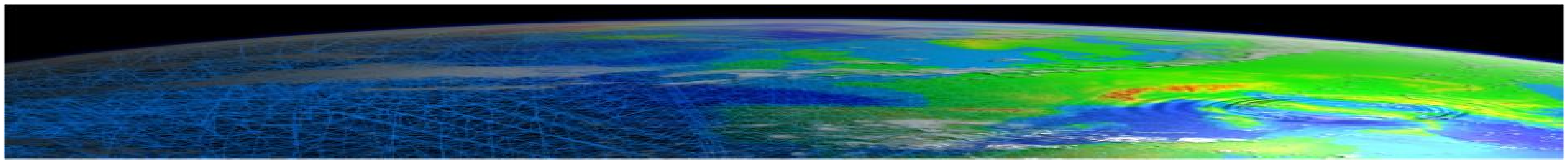

Goal and motivation

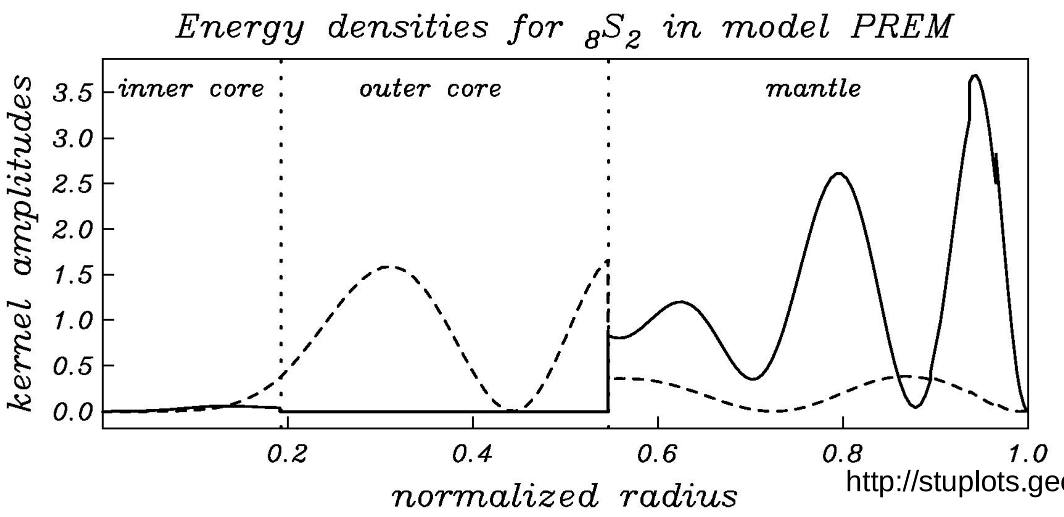

http://stuplots.geophys.uni-stuttgart.de/~plots/Modes/modes.html

Earth's structure determination

* key factor: density (ρ)

shear energy density

compressional energy density

Earthquake source studies

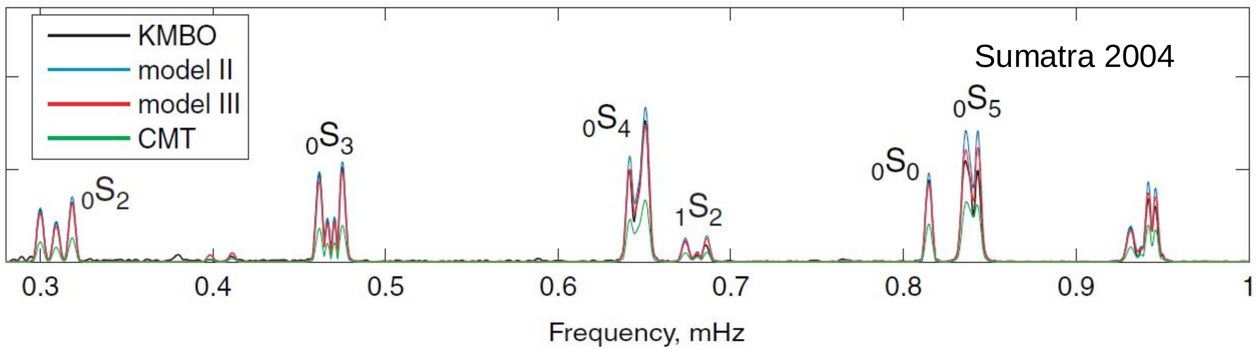

Park et al., (2005)

SOURCE MODEL DETERMINATION USING NORMAL MODES

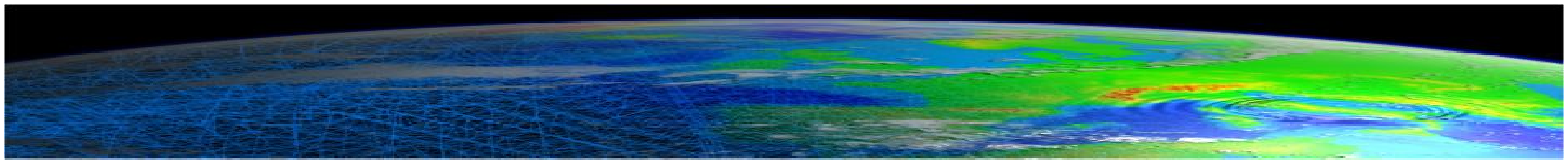

Summary

1. Testing existing global subduction earthquake source models

2. Probabilistic normal mode source model inversion

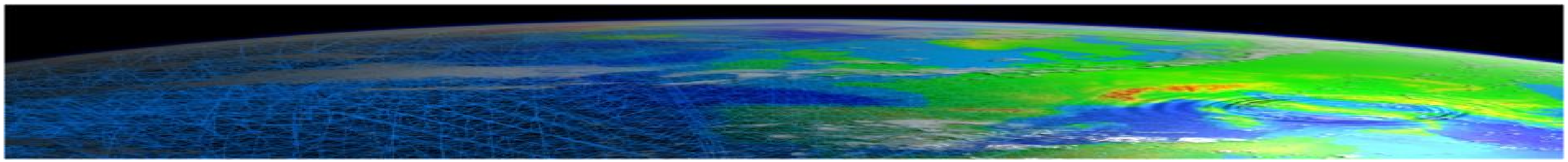

Summary

1. Testing existing global subduction earthquake source models

2. Probabilistic normal mode source model inversion

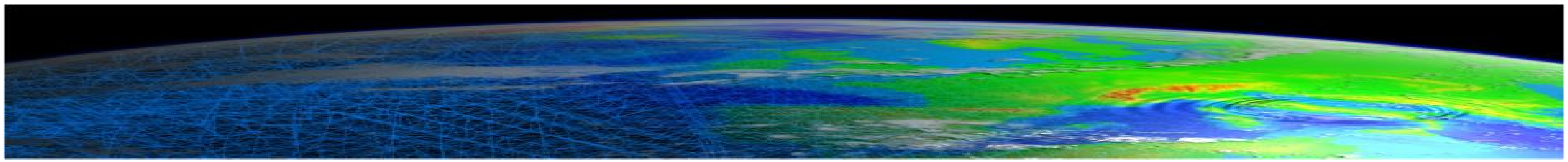

The GCMT and SCARDEC methods

- Semi-automated technique
- Long-period body-wave & surface-wave data (45 - 135 s)
- Point source approximation (centroid location)
- Time needed > 3h

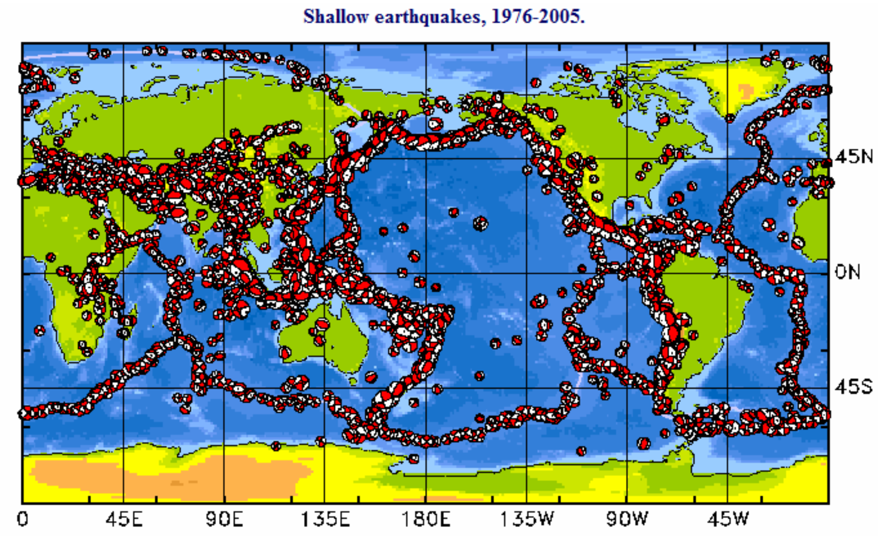

http://www.globalcmt.org/

- Automated technique
- Long-period body-wave data (33 - 200 s)
- Point source parameters & STF
- No location determination
- Time needed ~ 40 min

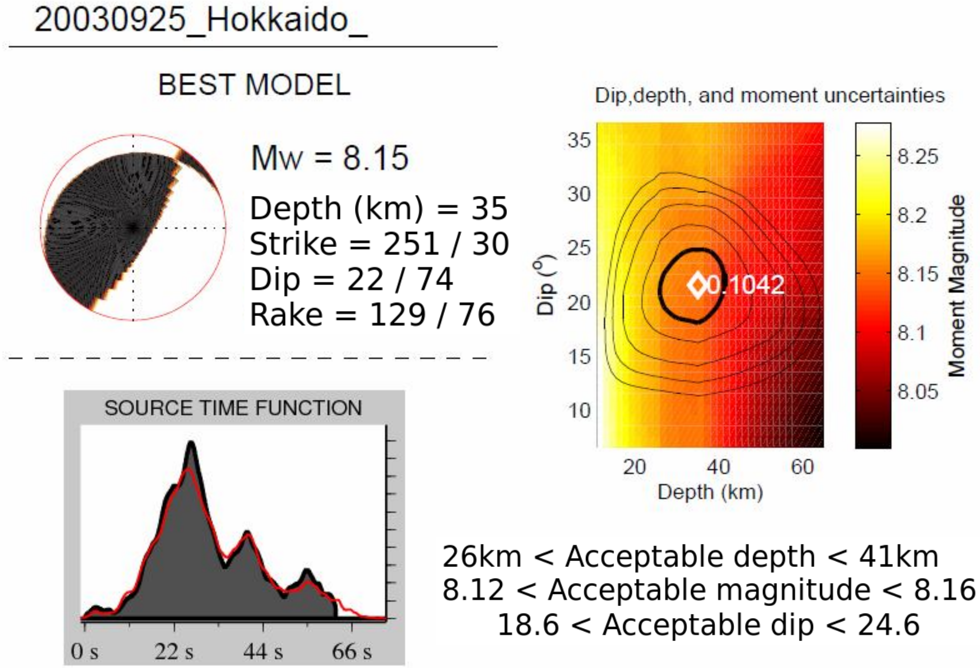

http://geoazur.oca.eu/SCARDEC

Vallée et al., (2010)

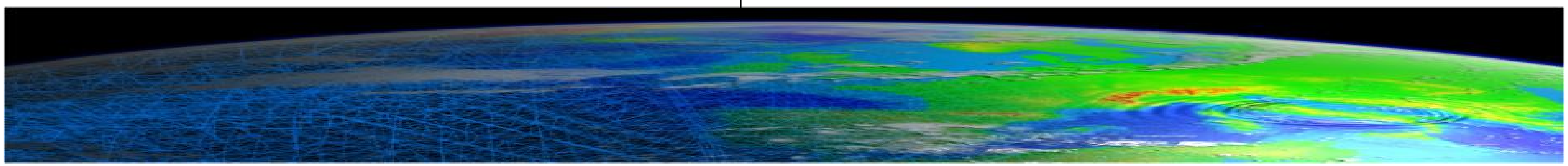

Subduction earthquakes studied

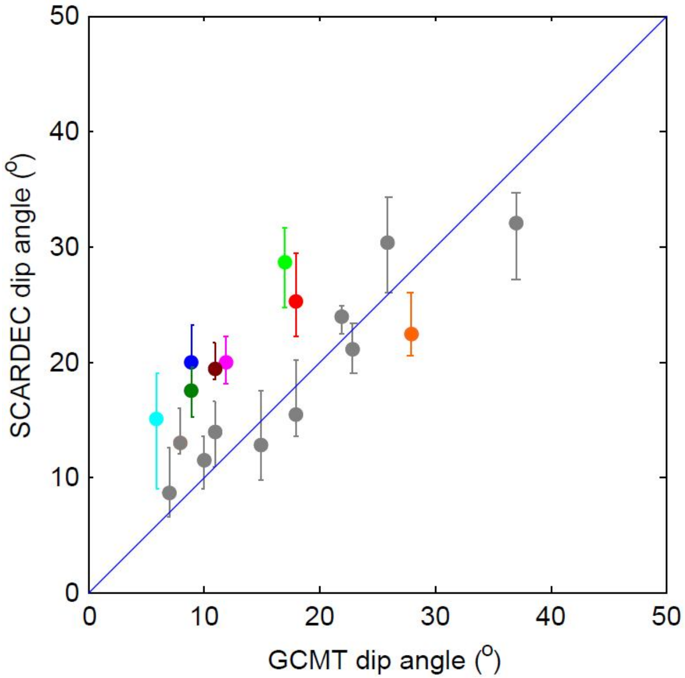

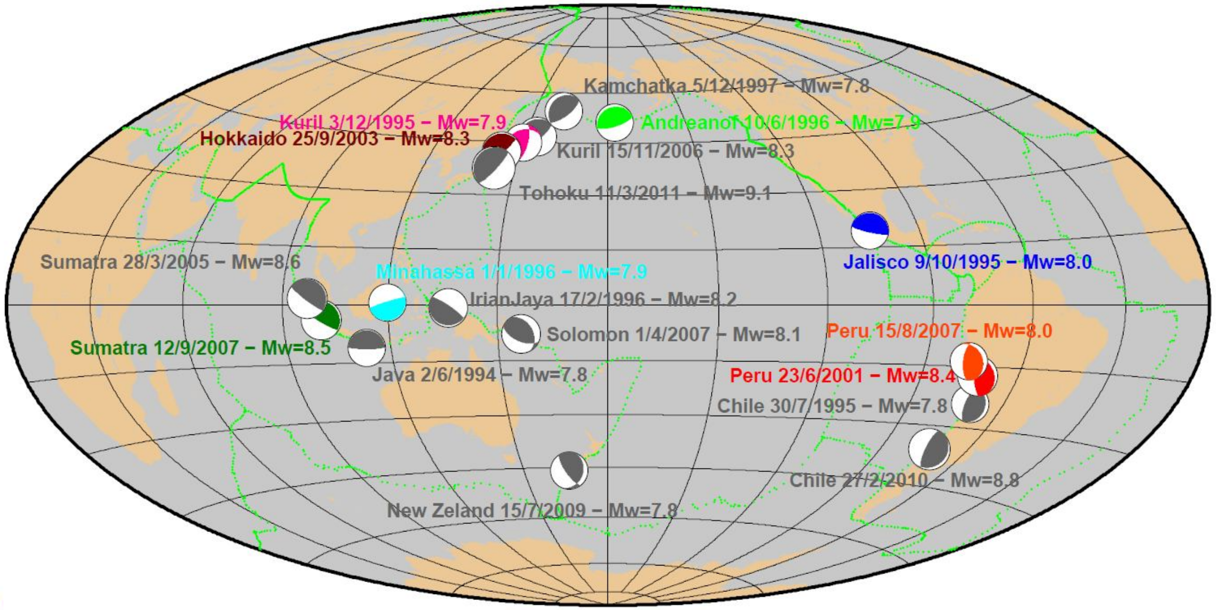

- M_w ≥ 7.8 subduction zone earthquakes over the last 20 years (Vallée et al., 2010)
- 8 selected earthquakes having large differences between GCMT and SCARDEC ($\Delta\delta_i \geq \Delta\delta^{average}$)

Lentas, Ferreira and Vallée, 2012 (in prep.)

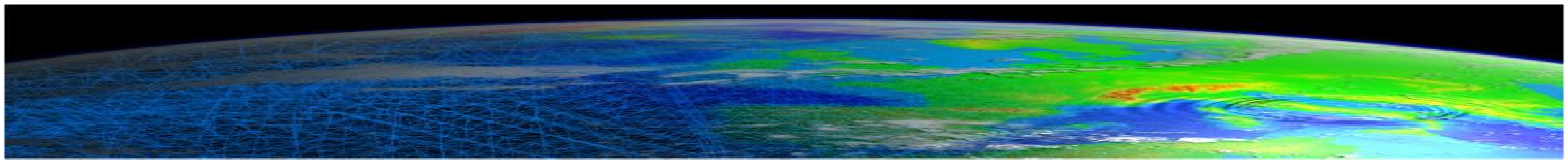

Normal mode spectra comparisons

Sumatra 2007

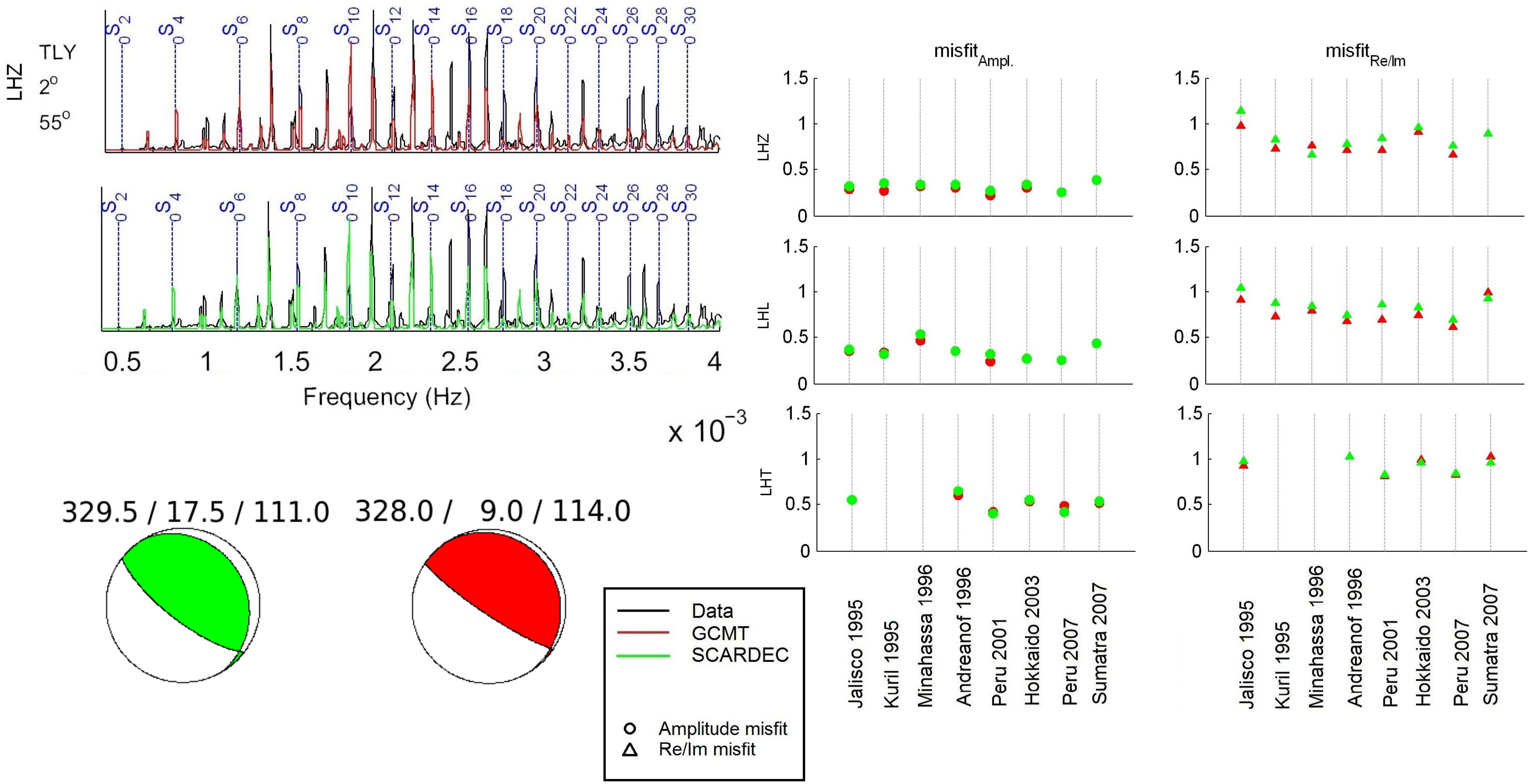

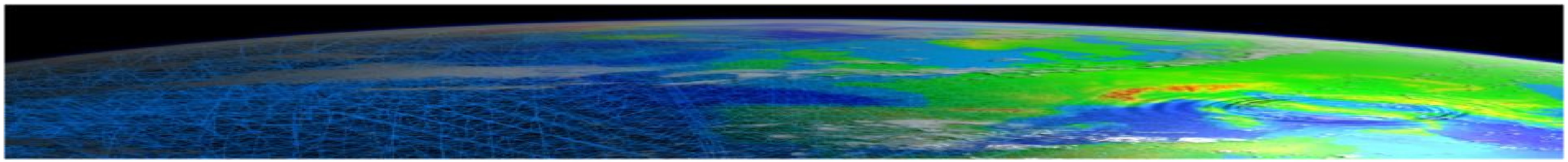

Body-wave comparisons

Peru 2001

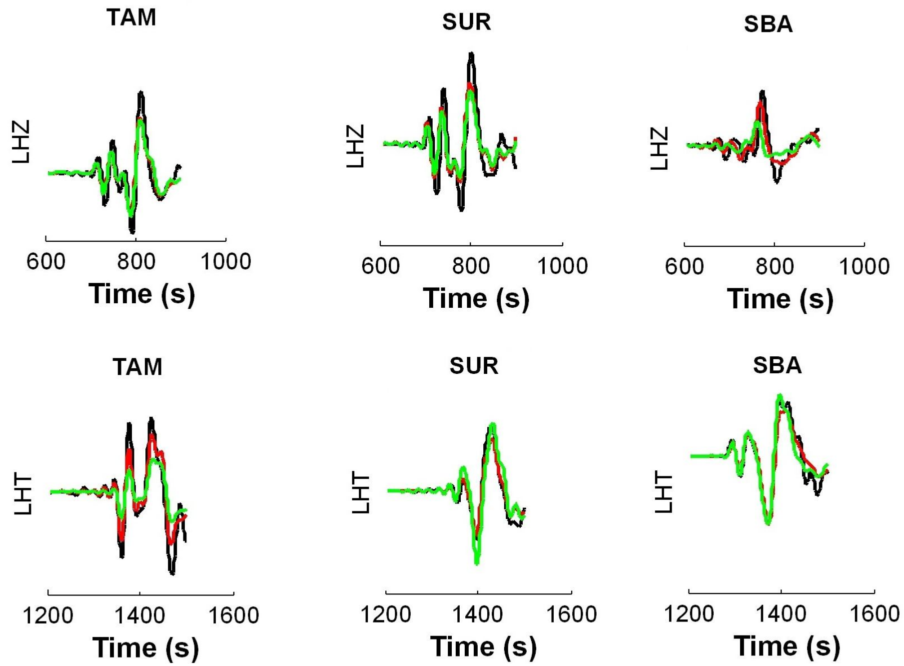

309.4 / 25.2 / 59.0

309.4 / 18.0 / 59.0

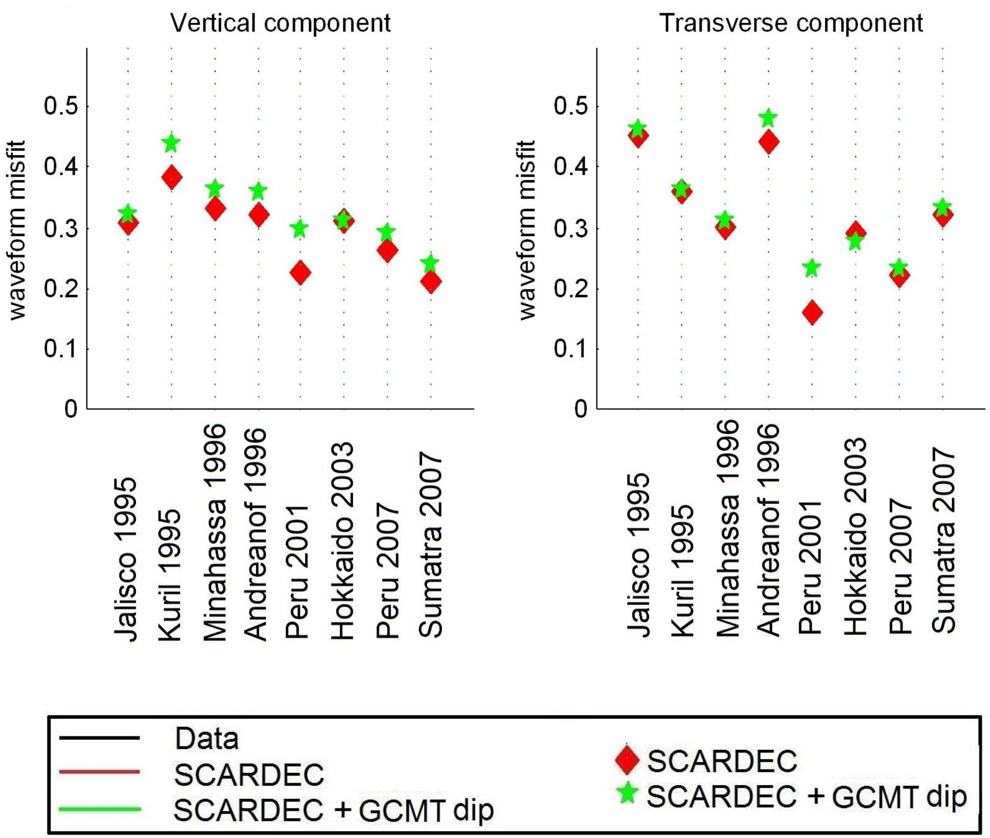

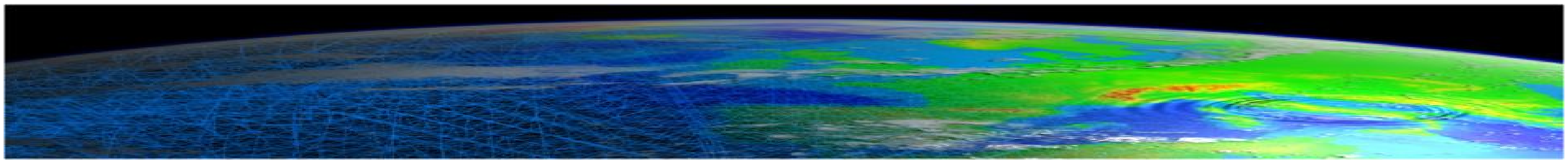

Comparisons with results taken from the literature

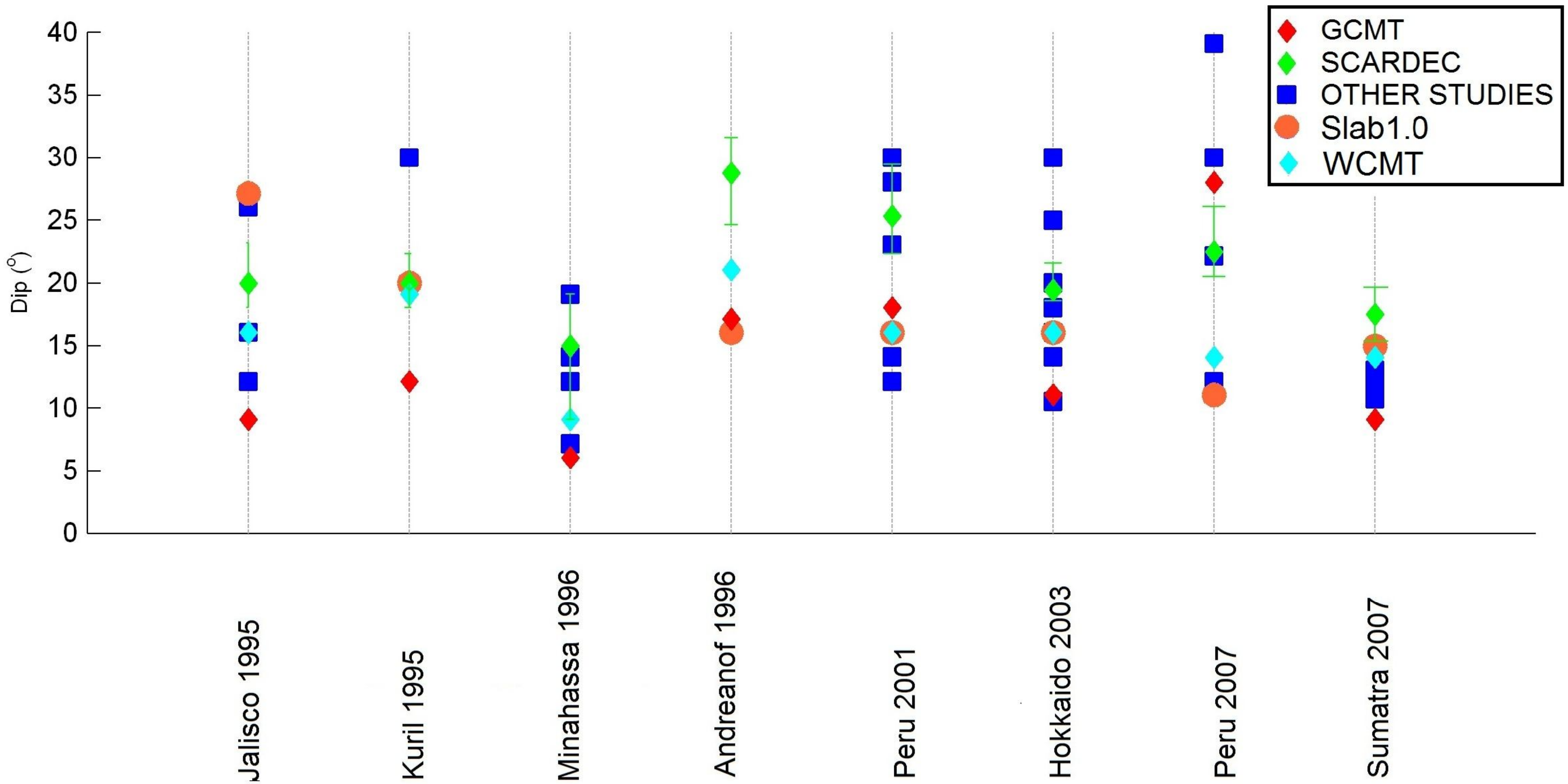

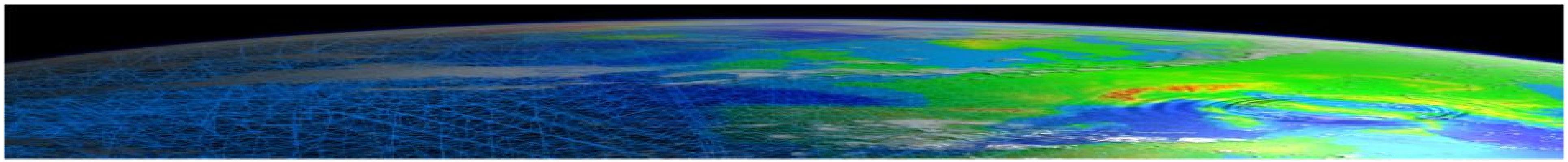

Summary

1. Testing existing global subduction earthquake source models

2. Probabilistic normal mode source model inversion

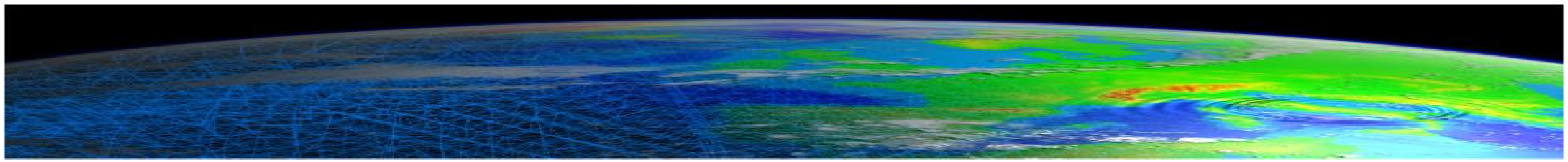

Finite source description

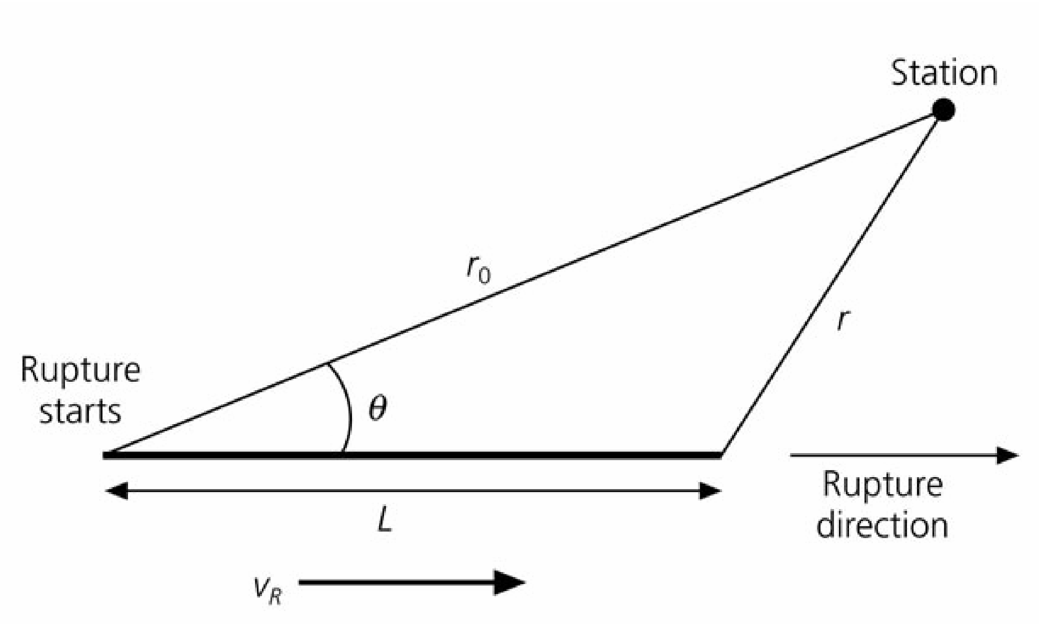

$$a_m^{fs}(x,t) = a_m^{ps}(x,t) * F_m$$

$$a_m^{fs}(x,\omega) = a_m^{ps}(x,\omega) \cdot F_m$$

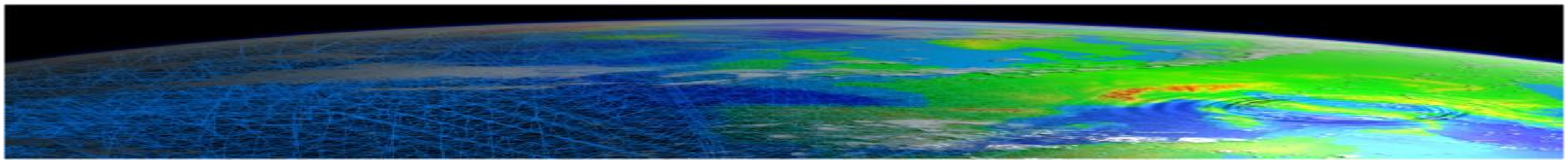

Finite source description

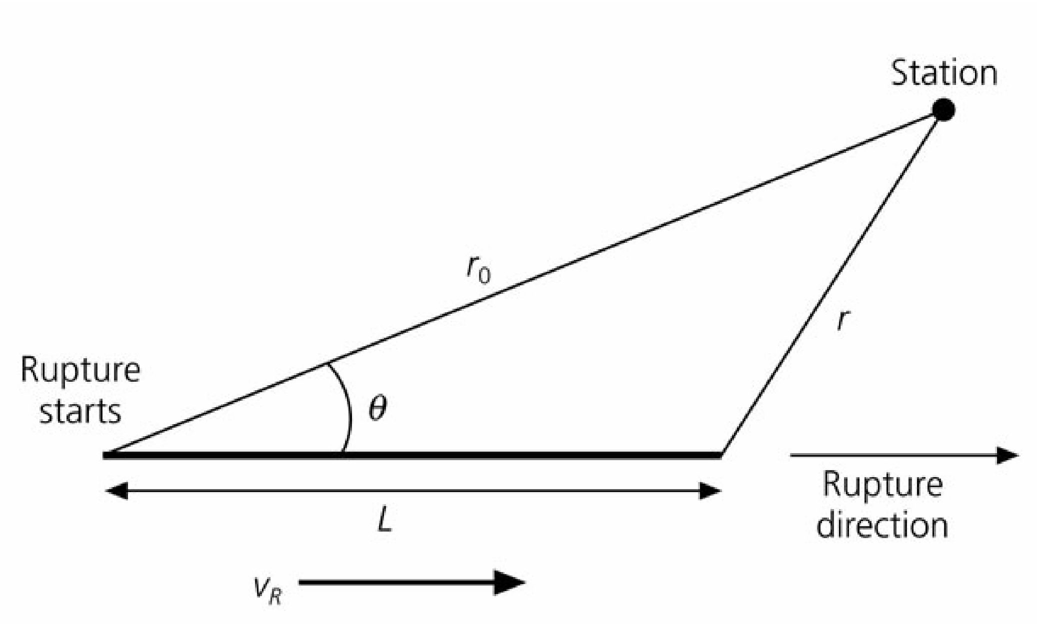

$$a_m^{fs}(x,t)=a_m^{ps}(x,t)*F_m$$

$$a_m^{fs}(x,\omega)=a_m^{ps}(x,\omega)\cdot F_m$$

$$x_m = f(L,T_r)$$

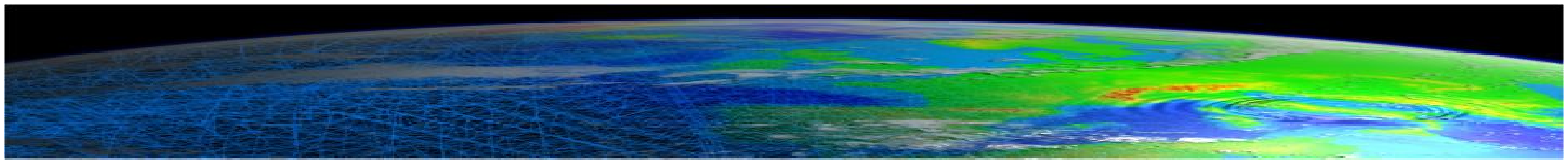

Synthetic test

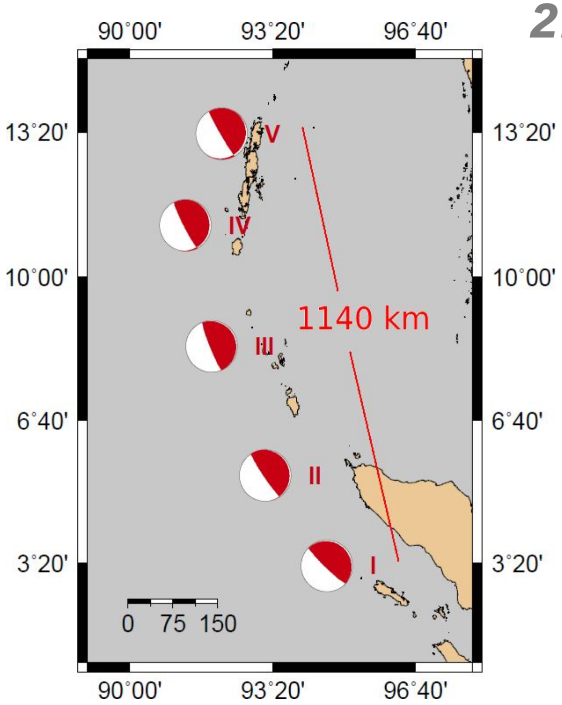

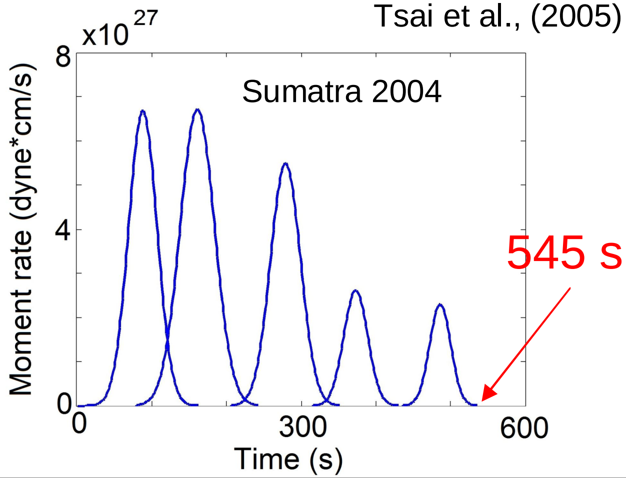

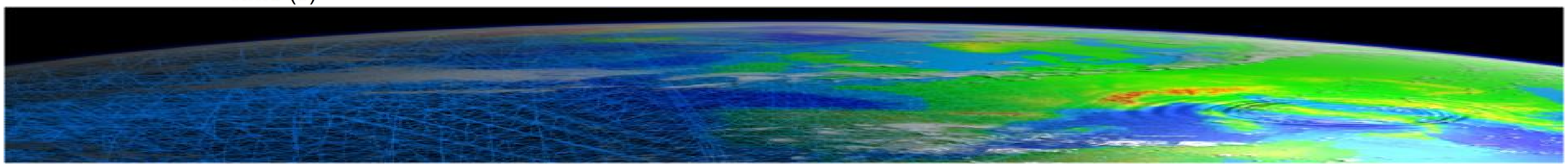

Synthetic test

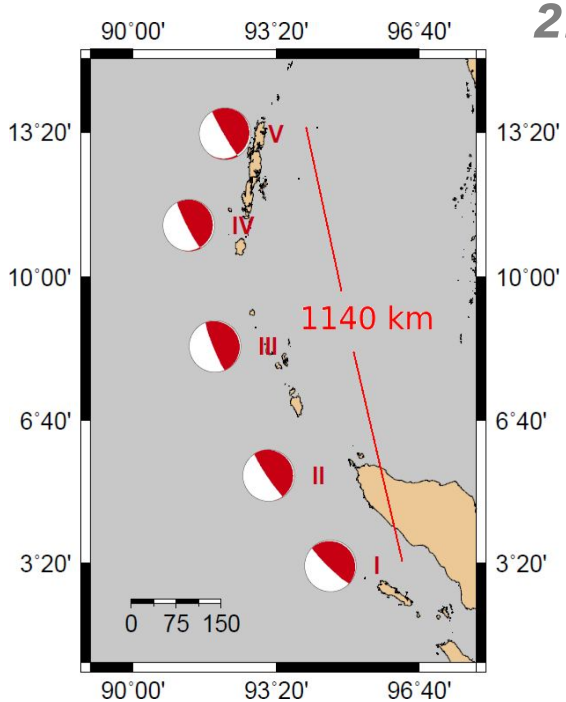

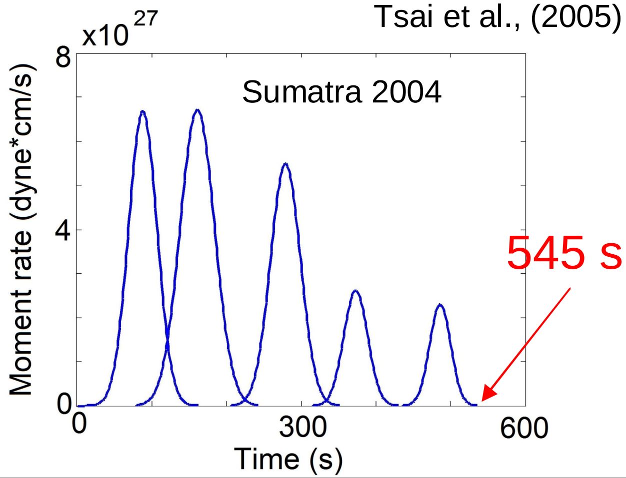

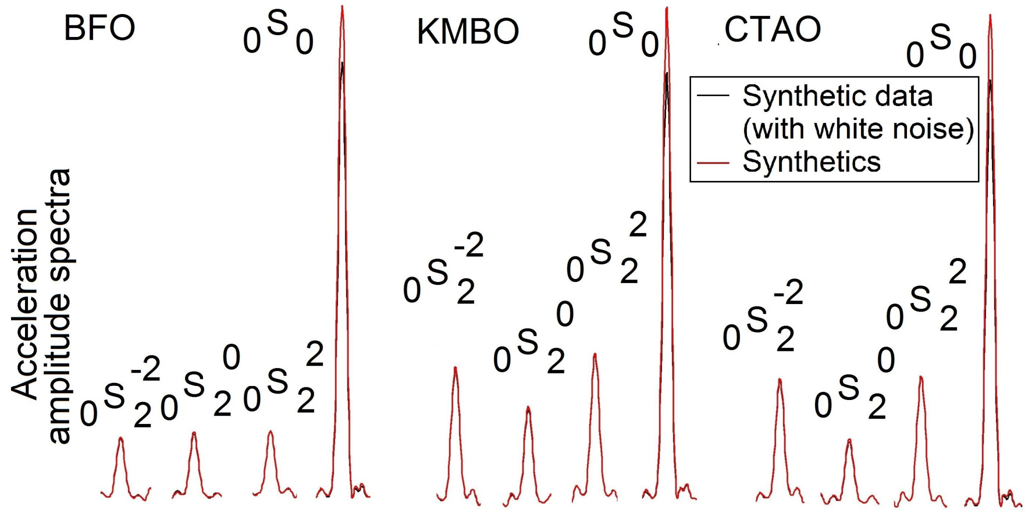

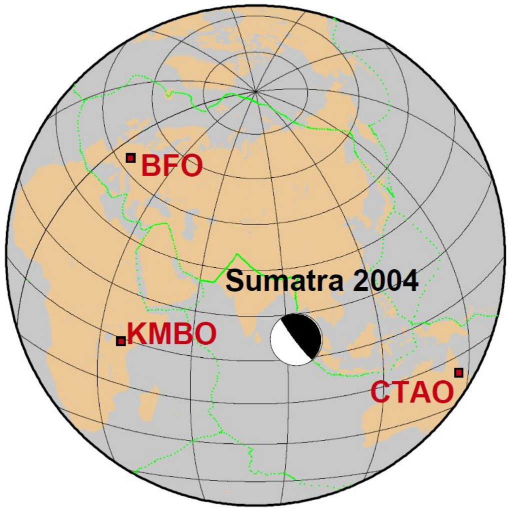

L = 1158.2 km

T_r = 549.1 sec

V_r = 2.1 km/sec

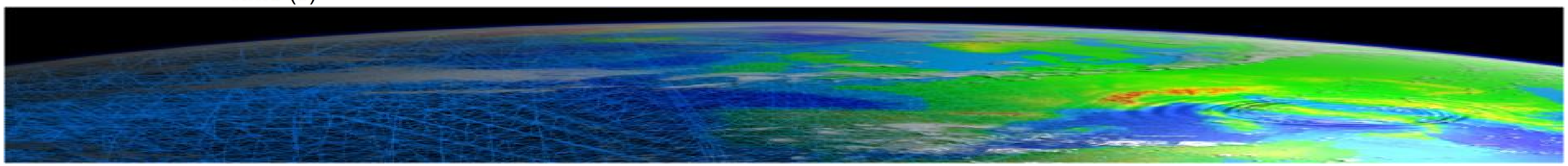

Sensitivity of the inversion to source parameters

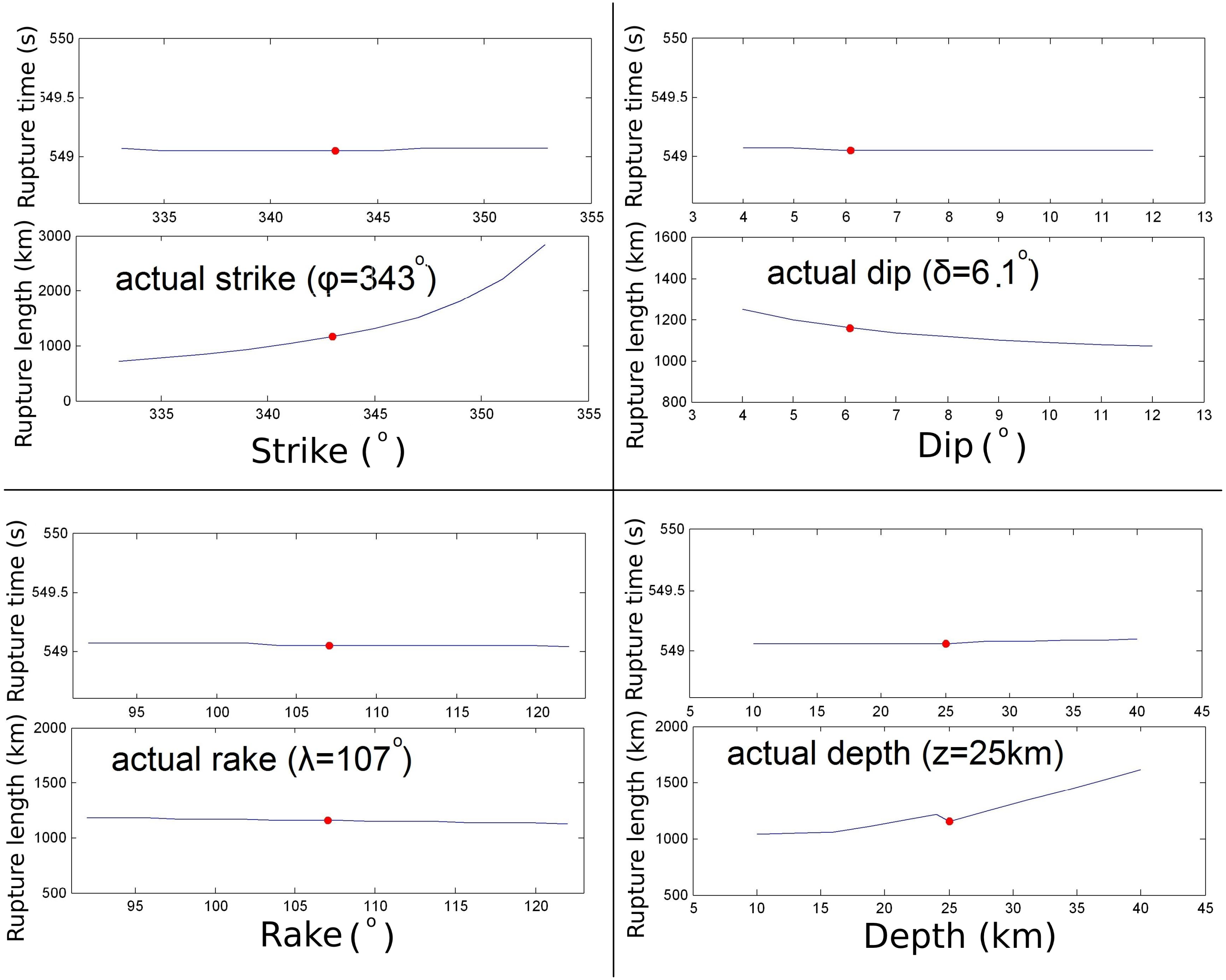

Sensitivity of the inversion to location

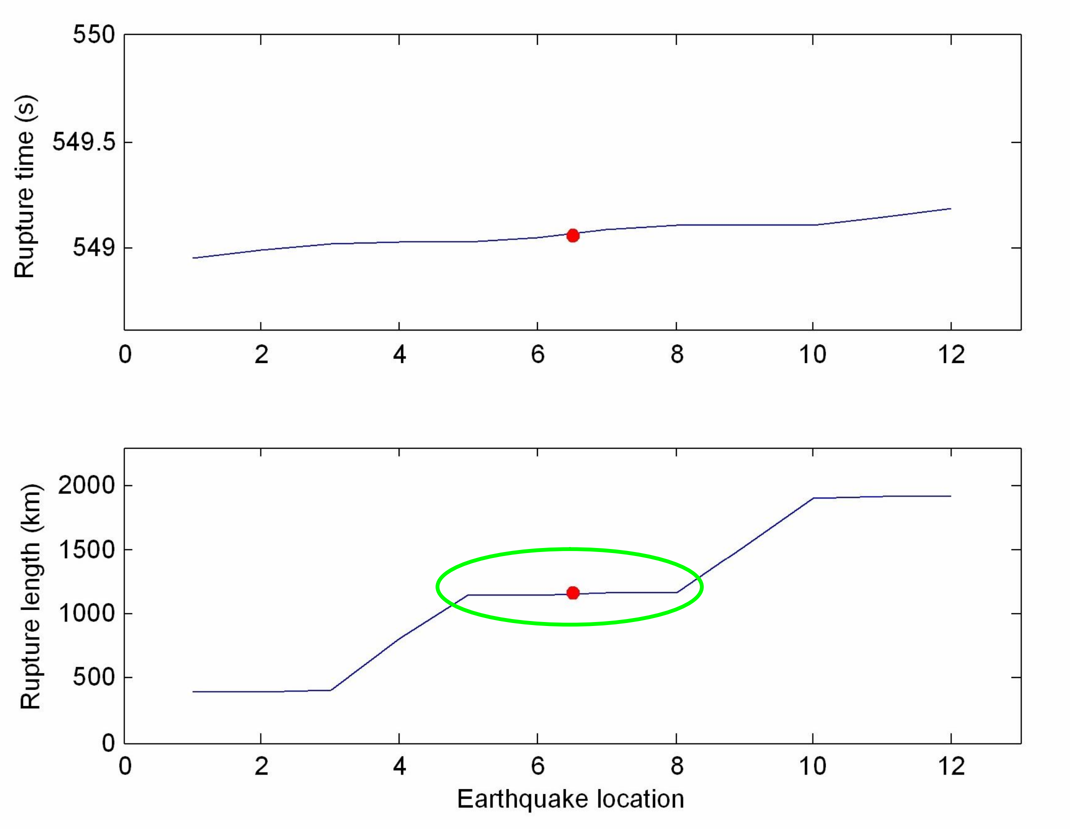

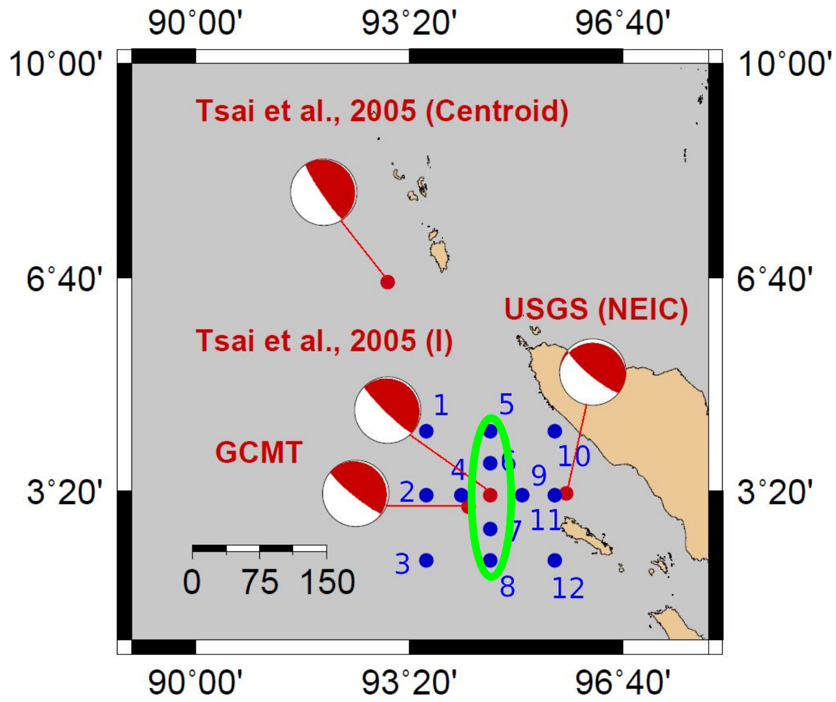

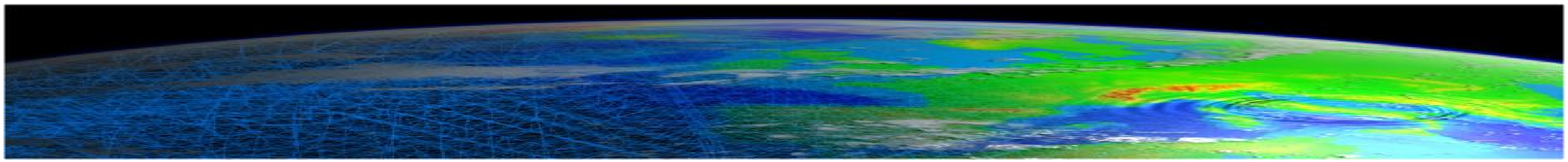

Sensitivity of the inversion to the Earth's structure

480 hours acceleration spectra (BFO)

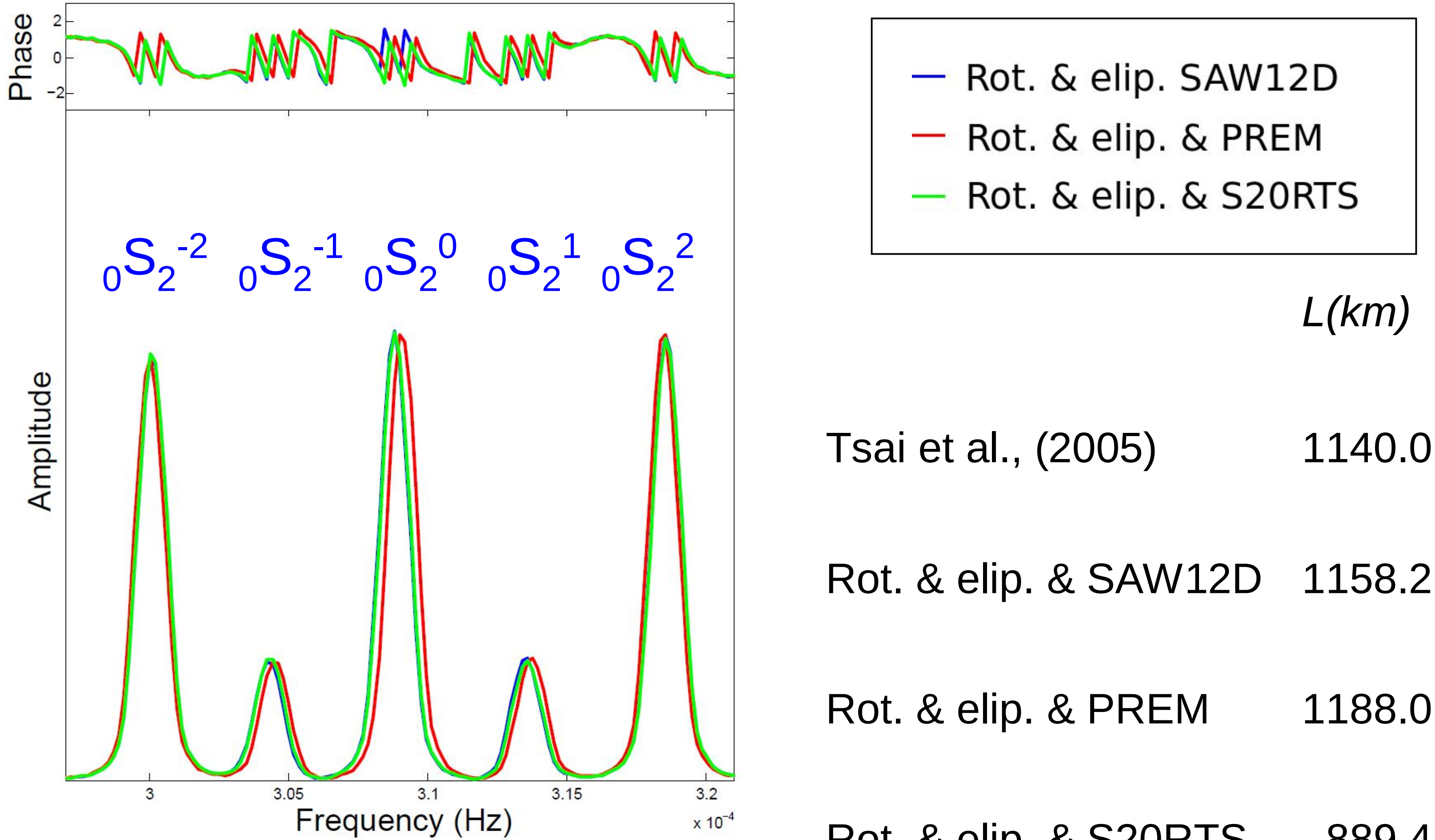

	L(km)	T_r*(s)*
Tsai et al., (2005)	1140.0	545.0
Rot. & elip. & SAW12D	1158.2	549.1
Rot. & elip. & PREM	1188.0	507.9
Rot. & elip. & S20RTS	889.4	603.9

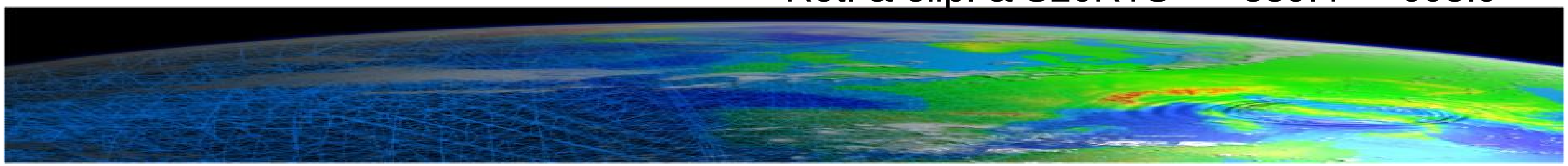

Probabilistic normal mode source inversion

Parameter space:
$(\varphi, \delta, \lambda, M_w, T_r, L)$

↓

Grid search
(N.A.)

→ Optimal source model

↓↑

Theoretical finite source spectra

L_2-norm misfit calculation between data and synthetic spectra

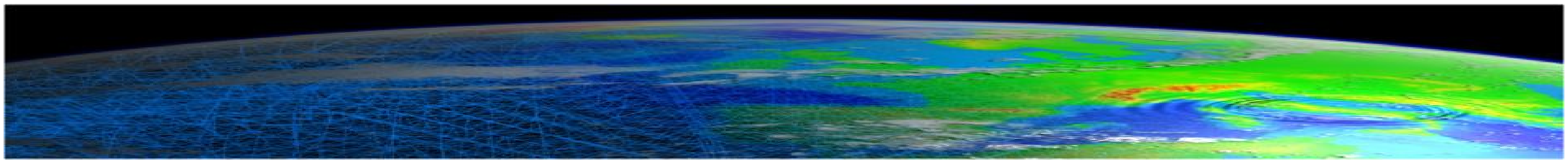

Probabilistic normal mode source inversion

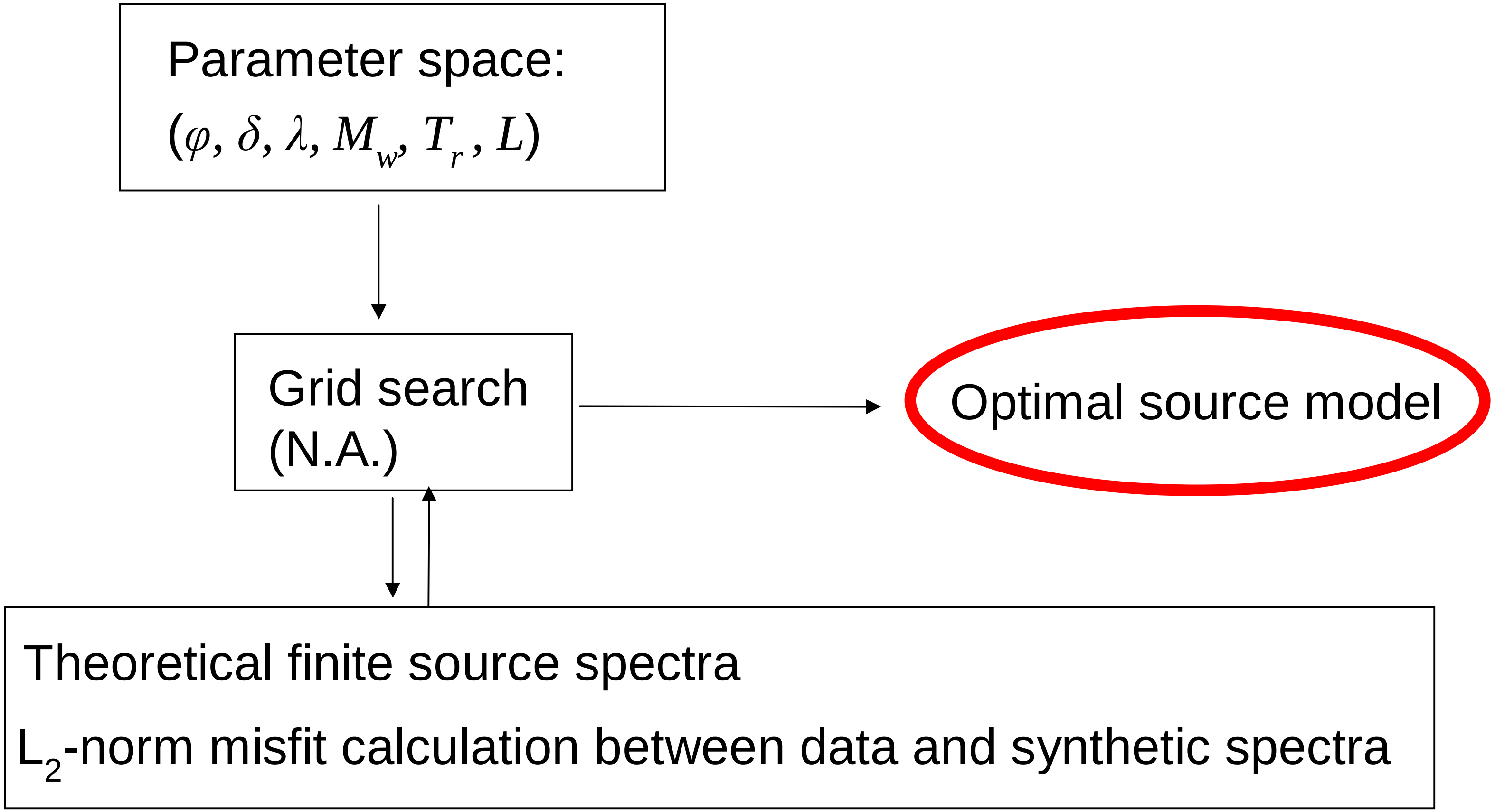

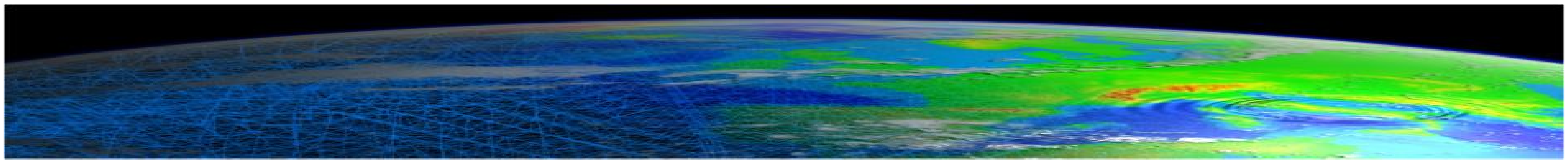

M_w 8.6 & 8.2 Sumatra 2012 earthquakes

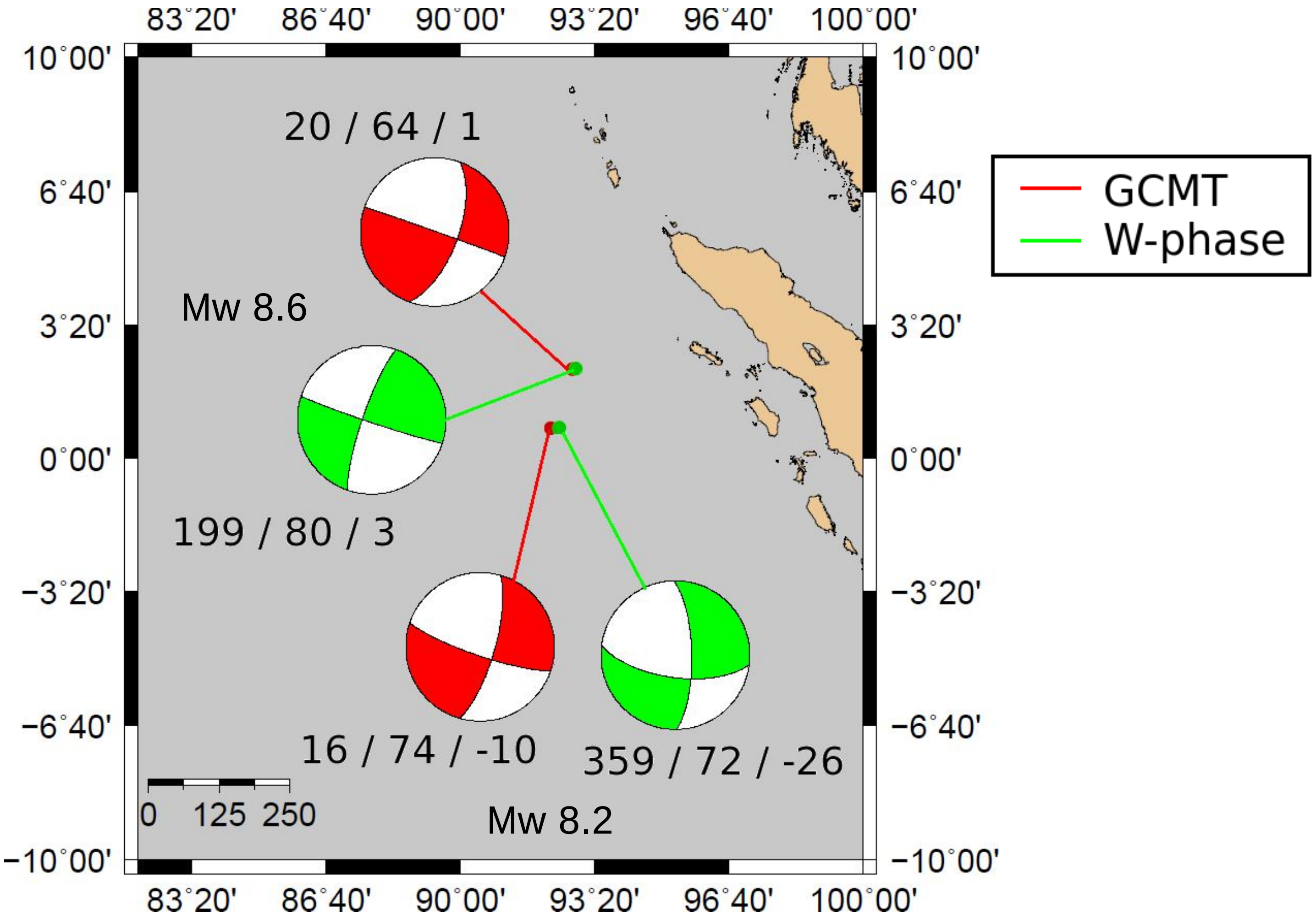

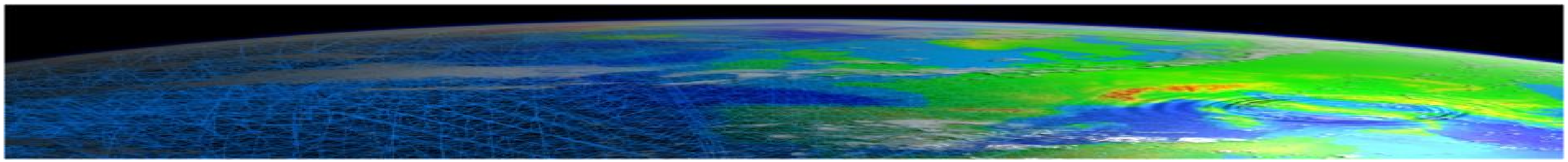

Sumatra 2012 normal mode spectra

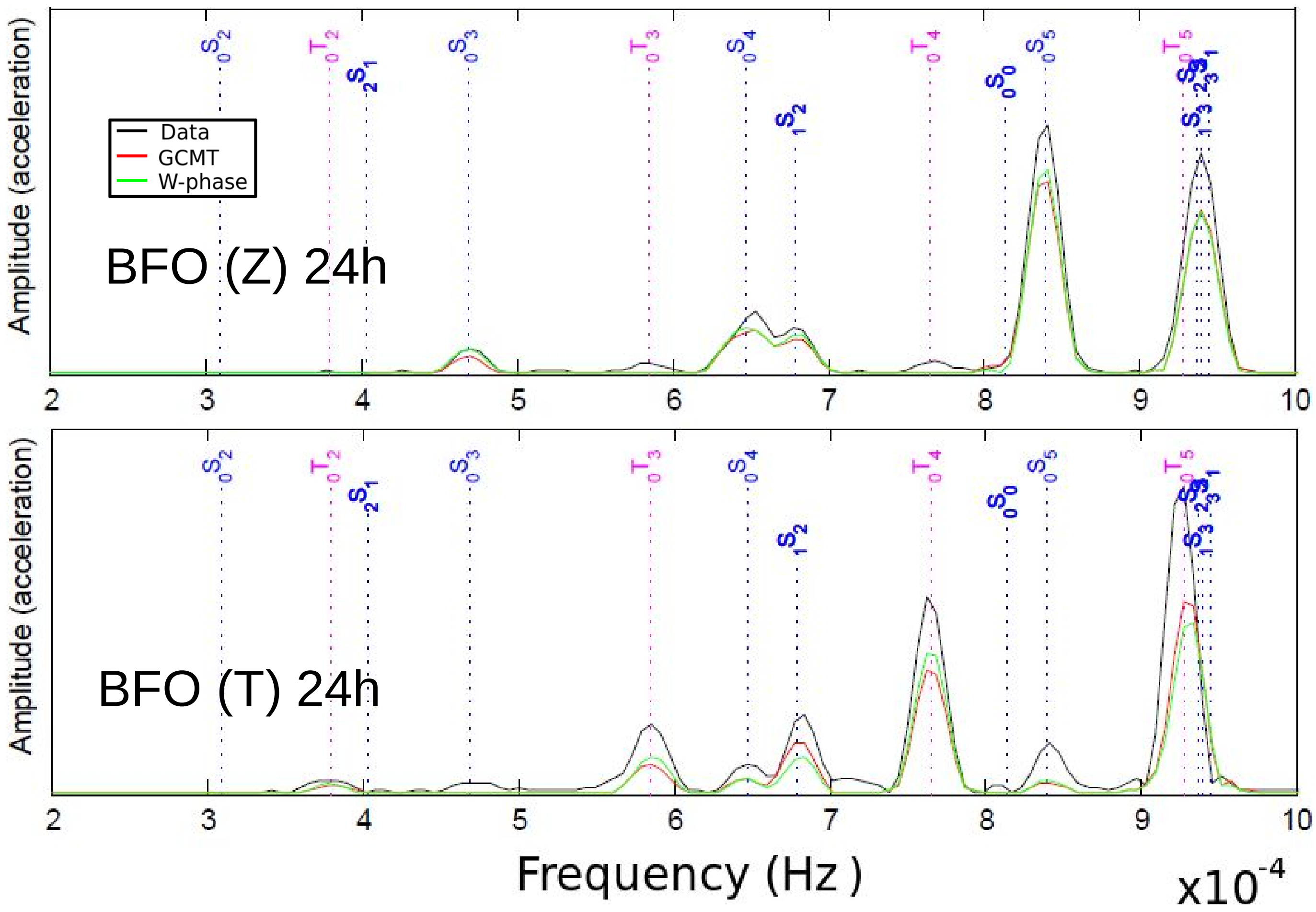

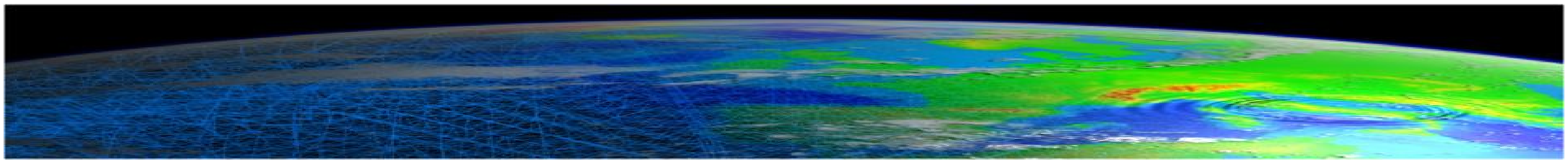

Sumatra 2012 normal mode spectra

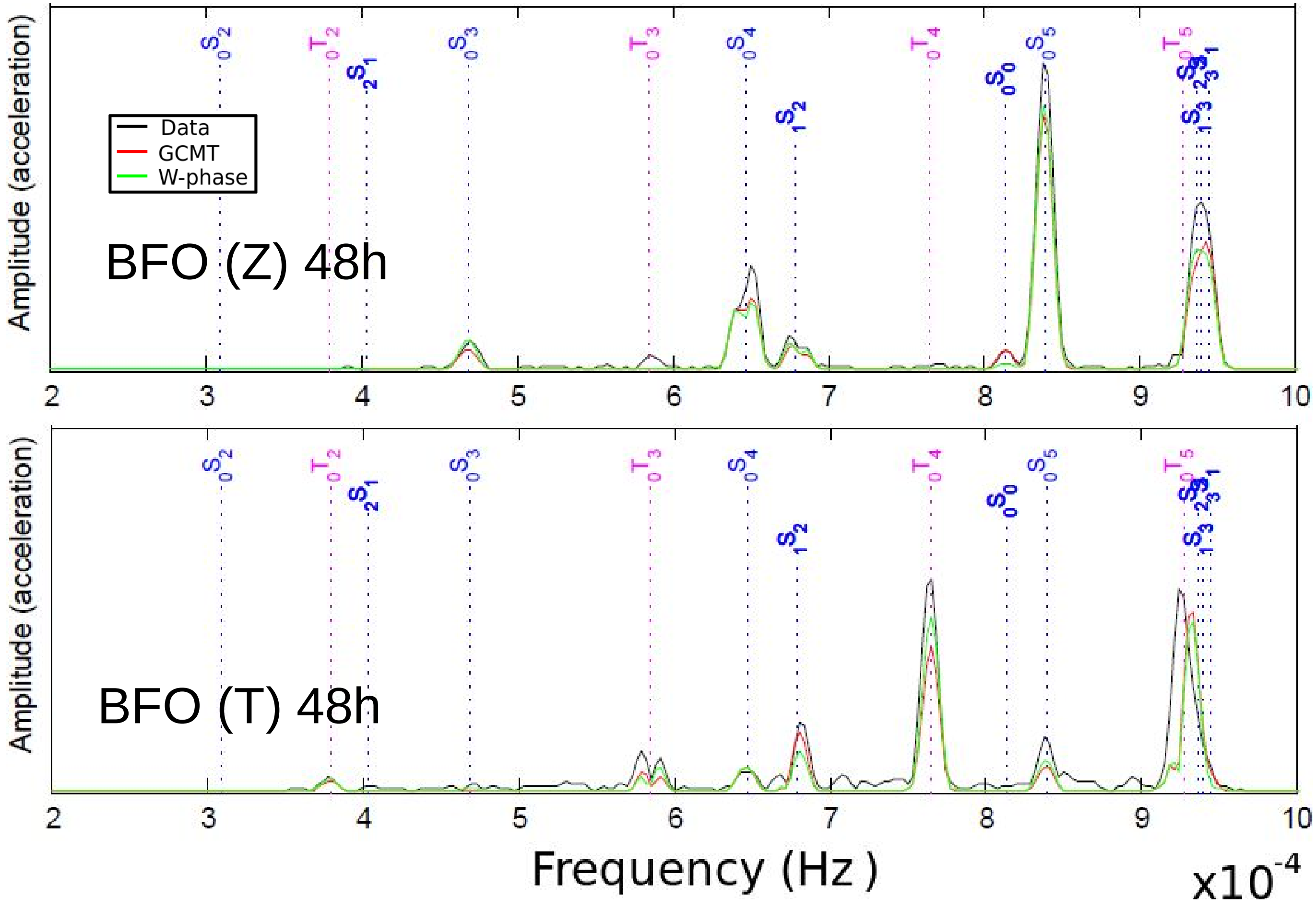

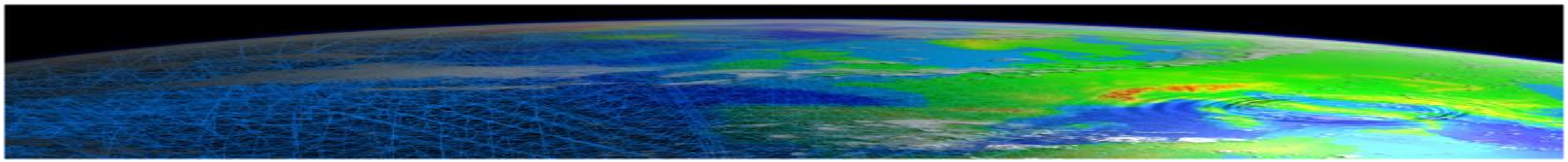

Sumatra 2012 normal mode spectra

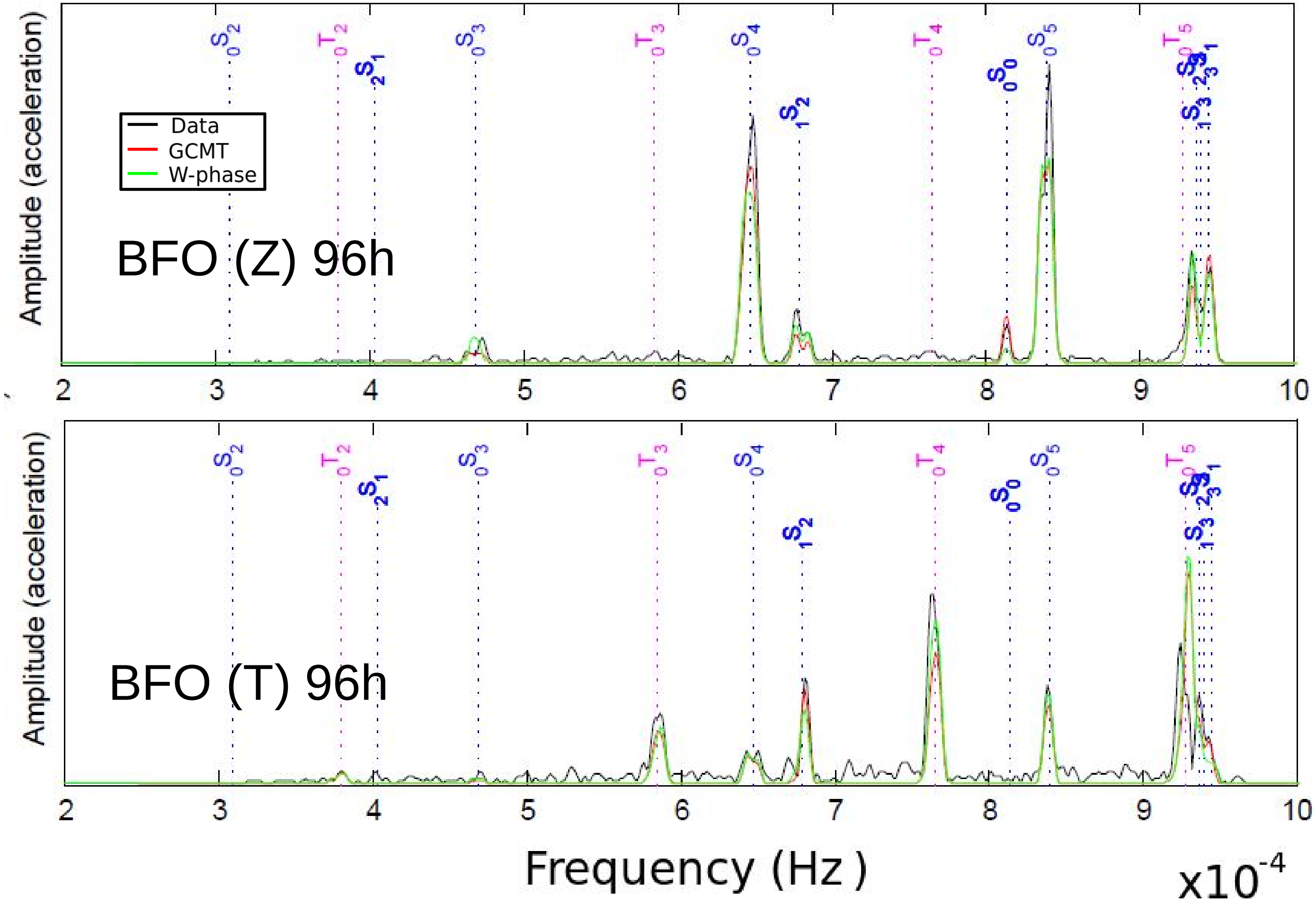

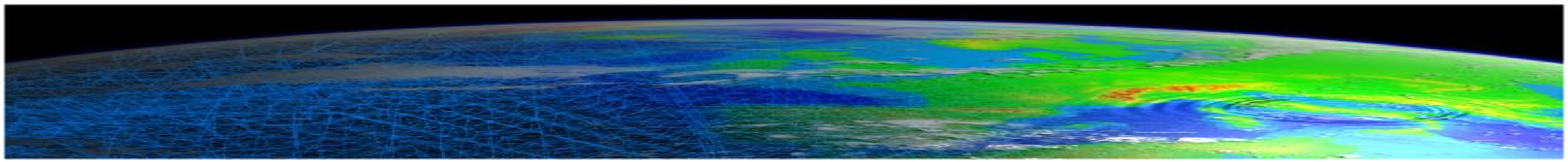

Sumatra 2012 normal mode spectra

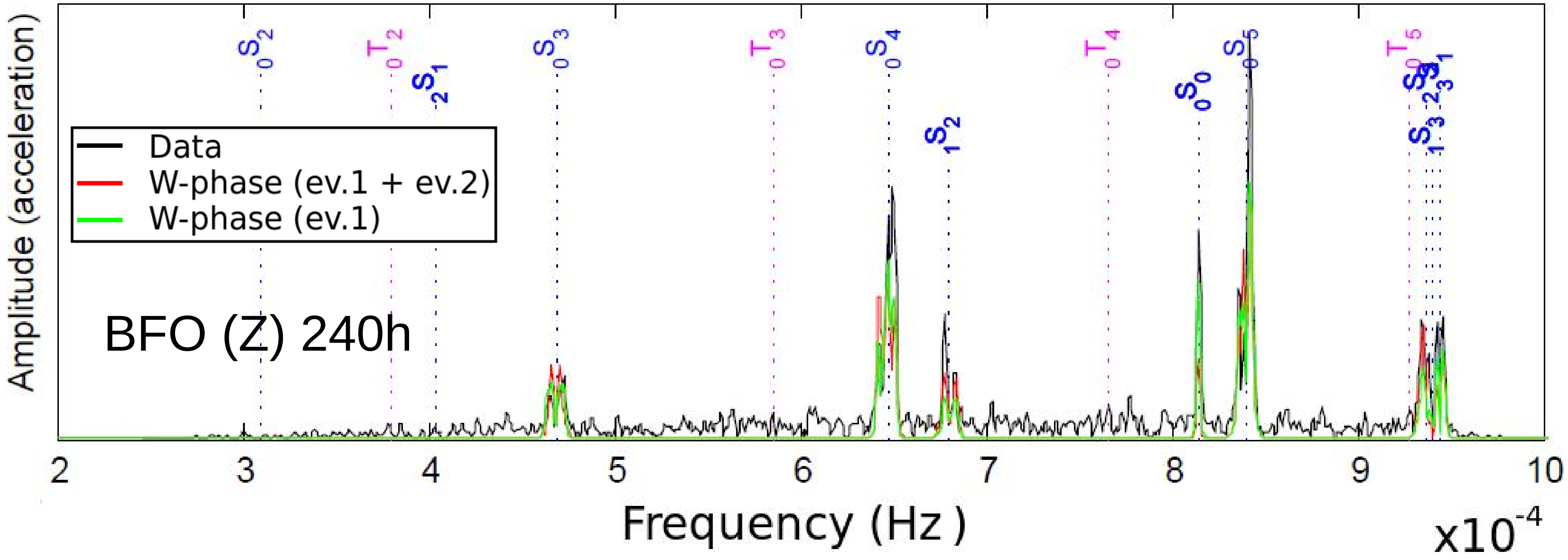

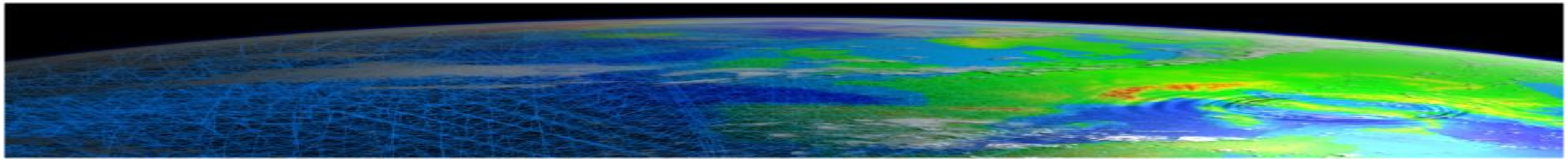

Sumatra 2012 normal mode spectra

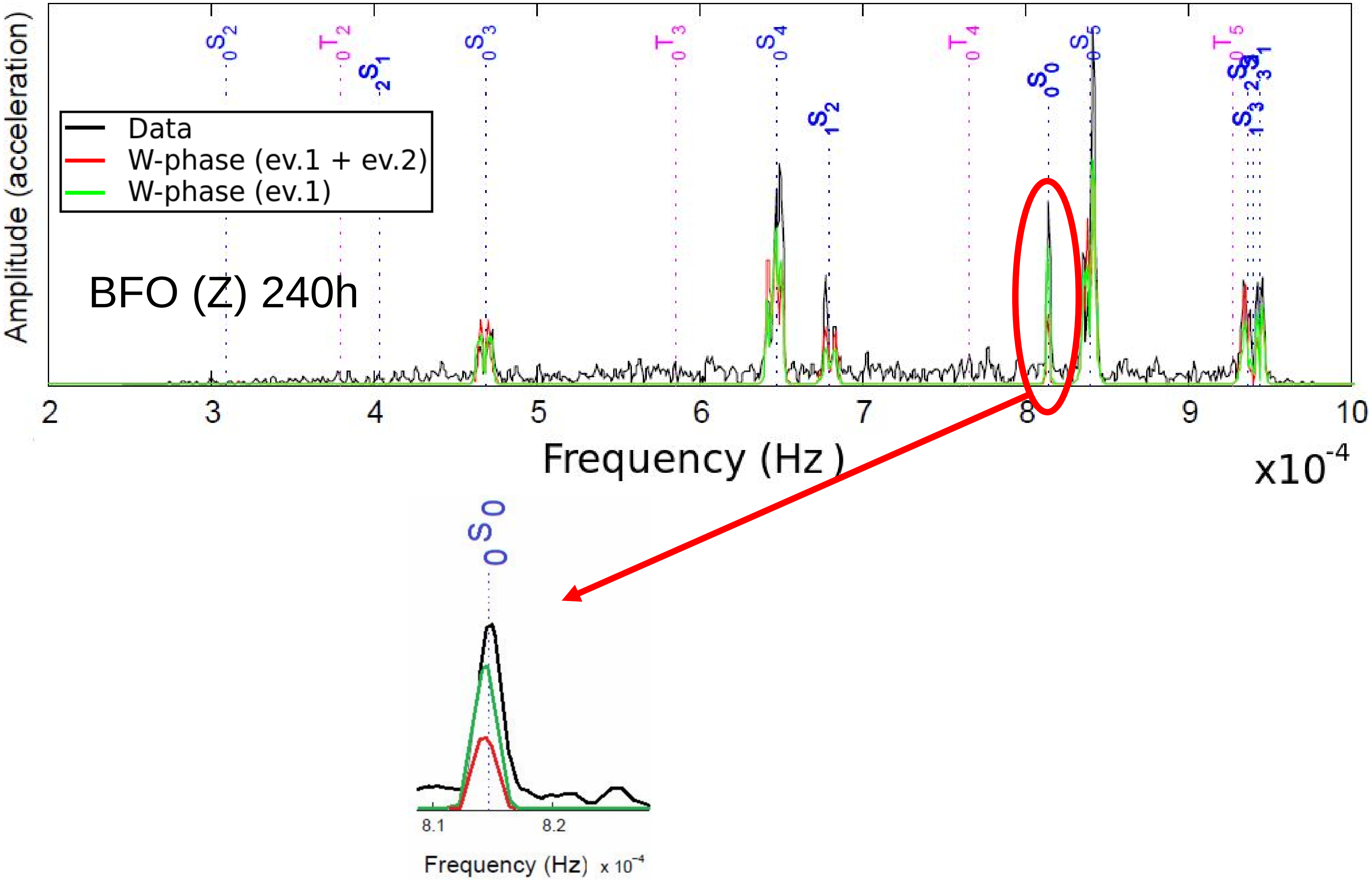

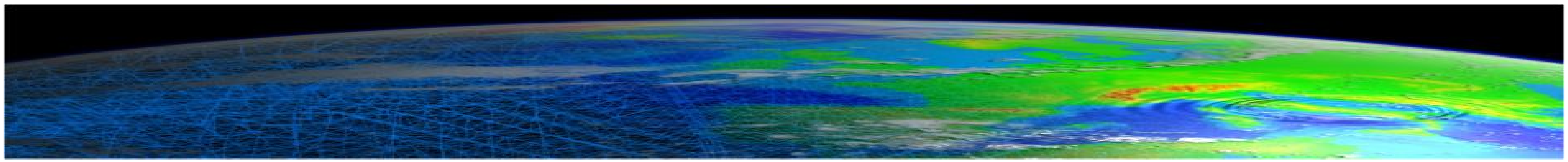

Conclusions

- The SCARDEC source parameters explain equally well the normal mode data compared to GCMT.

- Body-wave tests combined with source parameters published in the literature, suggest that the SCARDEC method determines the fault dip angle slightly better than GCMT.

- We developed a linear inversion code which determines the singlets' initial phases of split multiplets and from these measurements, the rupture time and length can be retrieved.

- Rupture length inversions are affected by the fault's strike and the location (epicentre, depth).

- 3D structure affects strongly both the rupture time and length.

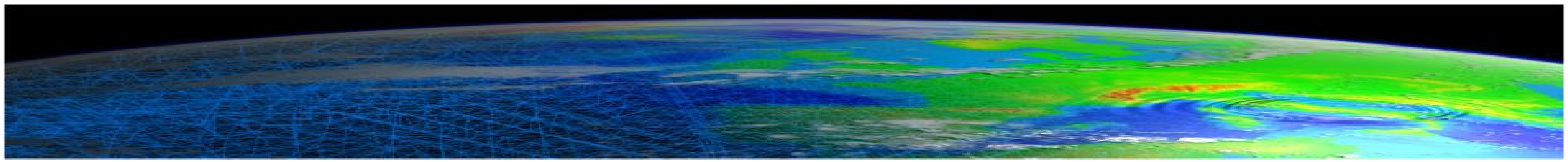

$$\alpha_{fs}^{m}(x,\omega) = \alpha_{ps}^{m}(x,\omega) \cdot F_m$$

$$\begin{bmatrix} d_{a_1}^j \\ d_{b_1}^j \\ d_{a_2}^j \\ d_{b_2}^j \\ . \\ . \\ d_{a_n}^j \\ d_{b_n}^j \end{bmatrix} = \begin{bmatrix} G_{a_1}^j & -G_{b_1}^j \\ G_{b_1}^j & G_{a_1}^j \\ G_{a_2}^j & -G_{b_2}^j \\ G_{b_2}^j & G_{a_2}^j \\ . & . \\ . & . \\ G_{a_n}^j & -G_{b_n}^j \\ G_{b_n}^j & G_{a_n}^j \end{bmatrix} \times \begin{bmatrix} Re(F_m) \\ Im(F_m) \end{bmatrix}$$

$$F_m = (G^T C_d^{-1} G)^{-1} G^T C_d^{-1} d$$

$$F_m = \frac{sin(X_m)}{X_m} e^{-iX_m}$$

$$X_m = \frac{\pi T_r}{T_m} + \frac{Lm sin(\phi)}{2r_o sin(\theta)}$$

$$\begin{bmatrix} X_{m_1} \\ X_{m_2} \\ . \\ . \\ X_{m_n} \end{bmatrix} = \begin{bmatrix} \frac{\pi}{T_{m_1}} & \frac{Lm_1 sin(\phi)}{2r_o sin(\theta)} \\ \frac{\pi}{T_{m_2}} & \frac{Lm_2 sin(\phi)}{2r_o sin(\theta)} \\ . & . \\ . & . \\ \frac{\pi}{T_{m_n}} & \frac{Lm_n sin(\phi)}{2r_o sin(\theta)} \end{bmatrix} \times \begin{bmatrix} T_r \\ L \end{bmatrix}$$

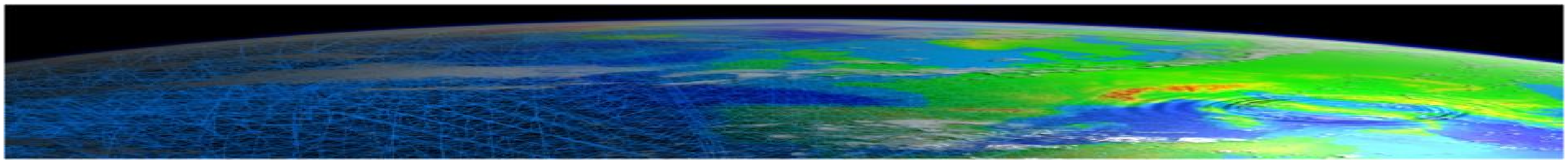

$$\alpha_{fs}^{m}(x,\omega) = \sum_{i=1}^{6} (\psi_i^m(x,\omega) \cdot M_i) \cdot F_m$$

$$\begin{bmatrix} \alpha_1^{ps} \\ \alpha_2^{ps} \\ . \\ . \\ \alpha_n^{ps} \end{bmatrix} = \begin{bmatrix} \psi_1^{(M_1=1)} & \psi_1^{(M_2=1)} & \psi_1^{(M_3=1)} & \psi_1^{(M_4=1)} & \psi_1^{(M_5=1)} & \psi_1^{(M_6=1)} \\ \psi_2^{(M_1=1)} & \psi_2^{(M_2=1)} & \psi_2^{(M_3=1)} & \psi_2^{(M_4=1)} & \psi_2^{(M_5=1)} & \psi_2^{(M_6=1)} \\ . & . & . & . & . & . \\ . & . & . & . & . & . \\ \psi_n^{(M_1=1)} & \psi_n^{(M_2=1)} & \psi_1^{(M_3=1)} & \psi_n^{(M_4=1)} & \psi_n^{(M_5=1)} & \psi_n^{(M_6=1)} \end{bmatrix} \times \begin{bmatrix} M_1 \\ M_2 \\ M_3 \\ M_4 \\ M_5 \\ M_6 \end{bmatrix}$$

$$\begin{bmatrix} \alpha_1^{ps} \\ \alpha_2^{ps} \\ . \\ . \\ \alpha_n^{ps} \end{bmatrix} = \begin{bmatrix} \frac{\partial a_1^{ps}}{\partial M_1} & \frac{\partial a_1^{ps}}{\partial M_2} & \frac{\partial a_1^{ps}}{\partial M_3} & \frac{\partial a_1^{ps}}{\partial M_4} & \frac{\partial a_1^{ps}}{\partial M_5} & \frac{\partial a_1^{ps}}{\partial M_6} \\ \frac{\partial a_2^{ps}}{\partial M_1} & \frac{\partial a_2^{ps}}{\partial M_2} & \frac{\partial a_2^{ps}}{\partial M_3} & \frac{\partial a_2^{ps}}{\partial M_4} & \frac{\partial a_2^{ps}}{\partial M_5} & \frac{\partial a_2^{ps}}{\partial M_6} \\ . & . & . & . & . & . \\ . & . & . & . & . & . \\ \frac{\partial a_n^{ps}}{\partial M_1} & \frac{\partial a_n^{ps}}{\partial M_2} & \frac{\partial a_n^{ps}}{\partial M_3} & \frac{\partial a_n^{ps}}{\partial M_4} & \frac{\partial a_n^{ps}}{\partial M_5} & \frac{\partial a_n^{ps}}{\partial M_6} \end{bmatrix} \times \begin{bmatrix} M_1 \\ M_2 \\ M_3 \\ M_4 \\ M_5 \\ M_6 \end{bmatrix}$$

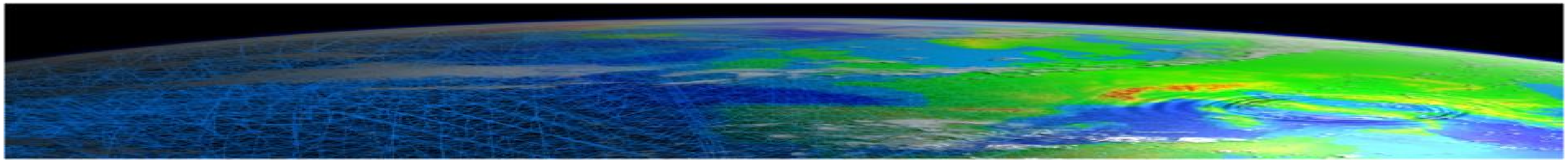

Synthetic test

Parameter space:

Strike	0.0	359.0
M_w	7.8	9.5
T_r	30.0	600.0
L	60.0	1440.0

Best fit model:

Strike	340.7º
Dip	6.1º
Rake	107.0º
M_w	9.3
T_r	555.5 s
L	1119.4 km

Input model:

Strike	343.0º
Dip	6.1º
Rake	107.0º
M_w	9.3
T_r	552.4 s
L	1153.9 km